BASE METAL MINERALIZATION IN THE KANMANTOO GROUP, S.A. : THE SOUTH HILL, BREMER AND WHEAL ELLEN AREAS

by

P. G. SPRY B.Sc.

Submitted as partial fulfilment of the Honours Degree of Bachelor of Science in Geology, at the University of Adelaide.

November, 1976

CONTENTS

FIGURES

TABLES

PLATES

ABSTRACT

The Kanmantoo Group in the Strathalbyn-Kanmantoo-Callington areas has been regionally metamorphosed and at least three deformations have affected the original greywacke - shale sediments to reach mid-amphibolite facies during the Delamerian orogeny. The metamorphic assemblages indicate a temperature of between 500 and 640°C and pressures between 1.8 and 3.8 kb. The presence of andalusite and fibrolite suggests pressures close to the upper value. Two deformations at quartz-muscovite-biotite grade followed, producing non-penetrative crenulation cleavages.

Evidence suggests that base metals were present in the schists at a very early stage either during sedimentation or introduced at least in the earliest stages of metamorphism, and to have been localized during the first deformation.

Sulphur isotope ratios of the sulphides are compatible with a hydrothermal origin and derivation from metamorphic fluids which had differing mixtures of meteoric, sea and possibly magmatic waters. Wide variations in isotope values between mineralization and pyritic schists and the Nairne Pyrite Formation suggest that the Cu-Pb-Zn was not derived from these pyritic horizons.

P-T conditions of sulphide recrystallization as derived from sphalerite geobarometry and sulphur isotopes indicate a temperature near 420°C and a pressure of 4.4 (±0.5) kb. The pressure is slightly higher than that deduced by silicate stabilities.

The andalusite schist is closely related to mineralization, not as a major source, but is structurally related being the lithology where folding and shearing were favourable for mineralization.

It is concluded that the mineralization is epigenetic, resulting from mobilization of disseminated sulphides in the country rocks by hydrothermal fluids into shear zones and tight folds.

Epigenetic – at or near the surface

1. INTRODUCTION

1.1 Nature of the Problem

A number of minor occurrences of base-metal mineralization occur within the regionally metamorphosed Kanmantoo Group on the south-eastern flank of the Mount Lofty Ranges between Kanmantoo (50 km east of Adelaide) and Strathalbyn (50 km south-east of Adelaide). The major Kanmantoo Mine has been studied in detail by Lindqvist (1969) and attention is concentrated in this study on the Wheal Ellen, Bremer and Strathalbyn Mines, the South Hill Prospect and the area around the Kanmantoo Mine itself.

1.2 Aims of the Investigation

The major aims are as follows:

(a) To describe the geology and mineralization of each of the minor deposits.

(b) To determine the relationship between metamorphism and mineralization.

(c) To compare the minor mineralization with that at the Kanmantoo Mine.

(d) To examine the possible genetic relationships between the mineralization and the andalusite schist, with which the mineralization is spatially associated.

(e) To attempt to determine the temperature and pressure conditions operating during metamorphism by the use of sphalerite geobarometry and sulphur isotope studies.

1.3 Previous Investigations

Studies in the general region include those of Grasso and McManus (1954), Kleeman and Skinner (1958), Offler (1960, 1963), Mirams (1962), Askins (1968), Offler and Fleming (1968), Lindqvist (1969), Poole (1969), Marlow (1975) and unpublished reports of Mines Exploration Pty. Ltd. and Northern Mining Pty. N.L.

Grasso and McManus (1954), Mirams (1962) and Poole (1969) discuss the general relationships of structure to mineralization in the Kanmantoo-Callington areas while details descriptions of the structural relationships are given for the Kanmantoo body (Lindqvist, 1969), and the Aclare Mine (Askins, 1968).

Syntheses of folding, metamorphism and stratigraphy of the Strathalbyn-Kanmantoo areas are given by Kleeman and Skinner (1958) and Offler and Fleming (1968). Offler (1960, 1963) and Marlow (1975) discuss structure, petrology and stratigraphy in the Strathalbyn area.

2. GEOLOGICAL SETTING

2.1 Regional Geology of the Kanmantoo-Strathalbyn Area

The Kanmantoo Group which is host to the mineralization consists of a thick succession of regionally metamorphosed pelites and greywackes of Cambrian age (Sprigg and Campana, 1953) overlying Proterozoic sediments of the Adelaide System (Daily and Milnes, 1972a; Marlow 1975) as in Fig. 1. The Group in general consists of mica-garnet-andalusite and quartz feldspar schists which belong to the almandine-amphibolite facies in the quartz-staurolite zone of regional metamorphism (Offler, 1960). The area studied is mainly the eastern limb of an anticline and minor folds are lacking.

All of the mineralized areas, with the exception of Bremer, lie in the Tapanappa Formation of the Inman Hill Sub-group of Daily and Milnes (1972a, 1973) about 1300 metres stratigraphically above the Nairne Pyrite Member. The Bremer Mine is located at a slightly higher stratigraphic level, just above the base of the Brown Hill Sub-group.

2.2 Local Geology of the Wheal Ellen and South Hill Areas

These areas are similar geologically and can be discussed concurrently. Detailed mapping was undertaken in both areas at a scale of 1:4000 using the lithologies described below, (see Figs. 2 and 3).

Quartz-mica schist is a massive, fine grained light to dark grey, weakly fissile quartz-rich schist varying in colour from light to dark grey which dominates both areas (See Figs. 2 and 3). Bedding 1 mm to several metres is reflected in variations in biotite and quartz content.

Biotite schist is a fine to coarse grained, light grey to black rock with a strong foliation consisting predominantly of biotite, quartz and muscovite with a few bands of staurolite, garnet and andalusite.

Andalusite schist is rich in andalusites up to 2 cm in length, in a biotite, muscovite, quartz, garnet host with minor staurolite and chlorite. The andalusites are commonly elongate parallel to the dominant schistosity. Andalusite-biotite interlayers are parallel to bedding, (see Plate 1a).

Two types of andalusite schist have been distinguished for mapping purposes. The first is characterized by large andalusite porphyroblasts and macroscopic layering. The second type contains small andalusites and is interlayered in biotite schist.

Dickinson (1942) considered that the andalusite schists within the Kanmantoo Group represented more intensely metamorphosed equivalents of the biotite schist. However, total rock analyses show that the

andalusite schists represent originally more aluminous layers compared with the mica schist, (see Table 1.)

Garnet-chlorite schist is the "Lode Schist" (Lindqvist, 1969) of the copper mineralization at Kanmantoo Mines. It is a medium grained garnet-chlorite-biotite-quartz schist with common coarse staurolite and minor andalusite. Garnet commonly constitutes greater than 60% of the rock. This unit is massive and has no dominant schistosity.

At South Hill mineralization is commonly associated with the garnet-chlorite schist whereas at Wheal Ellen this is not the case. The unit probably represents an original iron-rich pelite.

Pyritic Schist is a highly weathered and stained quartz sericite schist with coarse orthoclase and tourmaline but with large amounts of pyrite (up to 20%) and pyrrhotite. Analysis shows that it contains up to 2700 ppm Zn and 610 ppm Pb (see Fig. 13).

The pyritic schist units are good marker horizons and delineate large scale structural trends. Internally they are contorted and contain microfolds. The pyritic schist units probably represent sulphide-rich biotite schists (George, 1967). The chemical composition is compared to the Nairne Pyrite Formation in Table 1.

Calc-silicate schists occur as minor units and are discussed in Section 4.2.5.

Concordant and discordant quartz-veins from 1 mm to greater than 2 m in thickness are present. The concordant variety being the most common exhibit pinch and swell structures (See Plate 1b). The veins are milky white in colour and are up to 40 m in length. Calcite, tourmaline, hematite, pyrite, pyrrhotite, chalcopyrite are common constituents. The number and size of quartz veins increases in close proximity to the mineralized zones.

TABLE 1 ANALYSES OF ANDALUSITE SCHIST AND PYRITIC SCHIST

	(1)	(2)	(3)	(4)	(5)	(6)	(7)	(8)
SiO_2	64.73	60.55	61.81	60.72	60.64	58.88	37.53	47.63
Al_2O_3	15.64	17.73	16.97	12.90	17.32	19.52	31.73	14.29
Fe_2O_3	x10.60	x11.04			2.25	x13.38	x16.62	
FeO			+ 9.26	+ 4.89	3.66			
MnO	0.06	0.06	0.98	0.20	Tr	0.19	0.32	
MgO	3.20	3.36	3.17	3.64	2.60	3.86	5.95	2.69
CaO	1.58	1.35	0.00	1.99	1.54	0.37	0.76	1.59
Na_2O	1.43	1.14	0.25	2.57	1.19	0.20	0.19	1.72
K_2O	3.68	4.60	2.56	4.05	3.69	3.50	6.10	3.18
TiO_2	0.65	0.71				0.81	1.19	0.53
P_2O_5	0.12	0.13				0.12	0.39	
Cu	0.00	0.04				0.01	0.01	
Pb	0.01	0.00				0.02	0.01	
Zn	0.01	0.01				0.10	0.19	
FeS_2								16.13
Fe.947S								11.85
Total	101.71	100.72	95.00	90.96	92.89	100.96	101.00	99.61
*Loss	1.90	2.57				.75	.75	

x Fe measured as Fe_2O_3

\+ Fe measured as FeO

* Loss represents the sum of: H_2O^+, S, C, $Fe^{2+} \rightarrow Fe^{3+}$, H_2O^-

(1) and (2) Andalusite schist, South Hill - analyst P. Spry.

(3) Andalusite schist, Kanmantoo Mines - analyst Lindqvist (1969).

(4) Mica schist (Biotite schist) - analyst Lindqvist (1969).

(5) Typical shale (Pettijohn, 1957).

(6) and (7) Pyritic schist, Wheal Ellen - analyst P. Spry.

(8) Nairne Pyrite Member - analyst George (1967).

3. STRUCTURE

3.1 Introduction

South Hill Prospect is within an area covered by Poole in 1969. Since then the Highways Department has excavated highway cuttings which provide excellent outcrop for structural work. It is from these cuttings that most of the structural interpretations have been developed, (see Fig.4). Wheal Ellen structural features will also be discussed.

3.2 Bedding (So)

Bedding (So) is generally defined by compositional layering from less than 1 mm to 30 m in thickness. On the fine scale, layers alternately rich and poor in biotite produce a colour contrast within the quartz mica schist. On a larger scale, So is preserved as alternations of quartz mica schist with biotite schist. Metamorphic minerals define a layering which probably represents bedding. Andalusite schist layers up to 30 m wide define bedding at Wheal Ellen and South Hill (see Plate 1a) while garnet layers up to 2 cm thick within biotite schist also occur.

Fine quartz veins produced by metamorphic differentiation of the biotite schist which follow So are folded by the first deformation. Pyritic schists also define bedding.

Cross bedding has been observed with an angle of nearly 80° between topset and forset beds suggesting the cross beds have been deformed.

Wheal Ellen and the western half of South Hill are on the eastern limb of an anticline. The bedding orientation is constant and has a mean orientation of 184/66E at South Hill and 176/62E at Wheal Ellen (see Fig. 5).

3.3 The First Cleavage (S1)

For both areas the first cleavage (S1) is penetrative on all scales. The micas define a well developed slaty cleavage parallel to the axial plane of folds which range from millimetres to several metres in wavelength and amplitude. Andalusites are elongate parallel to S1 as are quartz veins with pinch and swell structure.

Poles to S1 are plotted for both areas, South Hill and Wheal Ellen, and have approximately the same orientation, (see Fig. 5).

3.4 So - S1 Intersection

Data from the highway cuttings at South Hill, where S1 has a constant orientation, indicate that the So - S1 intersection is parallel to the mineral lineation. This differs from the observations of Poole (1969) over a larger area. At South Hill the mean orientation is 52° to 088° and at Wheal Ellen it is 58° to 094°, (see Fig. 5).

TABLE 2 **STRUCTURAL NOMENCLATURE**

Deformations	Surface	Lineation	
Initial Structures	So - Bedding		
D1	S_1 - slaty cleavage and schistosity	L_1 - Lineation in S_1 d elongation of biotite, muscovite and andalusi	
D2	S_2 - axial plane of east-west crenulation, crenulation cleavage	L_2 - fold axis of crenulation	F_2 - crenulation in S_1
D3	S_3 - axial plane of north-south crenulation, crenulation cleavage	L_3 - fold axis of crenulation	F_3 - crenulations in S_1
D4	S_4 - axial plane of late stage kinks in S_1. Minor faults and cross-cutting veins.		

(So) bedding
(D1) - (S1) - slaty cleavage and schistosity
- (L1) - lineation in (S1) due to elongation of biotite
- (F1) - small folds and mesoscopic folds in (So)

(D2) - (S2) - axial plane of E-W crenulation - crenulation cleavage
- (L2) - fold axis of crenulation
- (F2) - crenulation in (S1)

(D3) - (S3) - axial plane of N-S crenulation - crenulation cleavage
- (L3) - fold axis of crenulation
- (F3) - crenulation in (S1)

(D4) - (S4) - axial plane of late stage kinks in (S1)
- minor faults and X-cut veins

3.5 Elongation in S1 (L1)

A mineral-lineation defined by the elongation of andalusite, muscovite, biotite, quartz rods and pseudo pebbles occurs in S1 in the schists. Andalusites up to 1 cm and biotites occur together as does fibrous muscovite and biotite.

At Wheal Ellen a quartz mica schist outcrop contains quartz rods 0.5 cm in diameter and 4 cm in length parallel to the mineral lineation. Pseudo pebbles up to 6 cm long commonly have this preferred orientation (see Plate 1d.) The "pebbles" are sandy layers within the quartz biotite schist in both areas.

The mineral lineations have similar mean orientations to the So - S1 intersection.

3.6 Crenulation Cleavage (S2) and Crenulation Lineation (L2)

A non-penetrative crenulation cleavage is developed parallel to the axial plane of the crenulation in the schists (particularly the pyritic schist). This cleavage is defined by quartz in the hinges and muscovite or a muscovite-biotite intergrowth in the limbs, (see Plate 3).

The mica flakes are recrystallized as indicated by polygonal apices. The symmetrical crenulation ranges in wavelength from 0.2 to 4 mm while the amplitude is between 1 mm and 8 mm. The larger wavelength and amplitude of the crenulation occur in the pyritic schist.

The mean orientation of the crenulation lineation is 58° to 099° at South Hill and 60° to 097° at Wheal Ellen, (see Fig. 5). No larger scale F2 folds other than F2 crenulations were observed.

Lindqvist (1969) and Poole (1969) considered the mineral lineation (L1) and the crenulation lineation (referred to here as L2) to be produced in the same deformational event. The mean orientations, for the two lineations, are clearly different; in one outcrop, where both were present an 18° difference in pitch was observed.

3.7 Crenulation Cleavage (S3) and Crenulation Lineation (L3)

A second crenulation at South Hill also develops a non-penetrative crenulation cleavage (S3). The wavelength ranges from 1 cm to 5 cm and the amplitude is about 1 cm. Fine scale crenulation is present but is relatively uncommon. As with the S2 crenulation, quartz concentrates in the hinge and biotite-muscovite in the limbs. The mean orientation of the crenulation lineation is 35° to 170°.

Class 1a mesoscopic F3 folds (Ramsay, 1967) are present also within the biotite schist at South Hill.

3.8 Kink Planes (S4)

Kinks were found only at Wheal Ellen but they have been reported

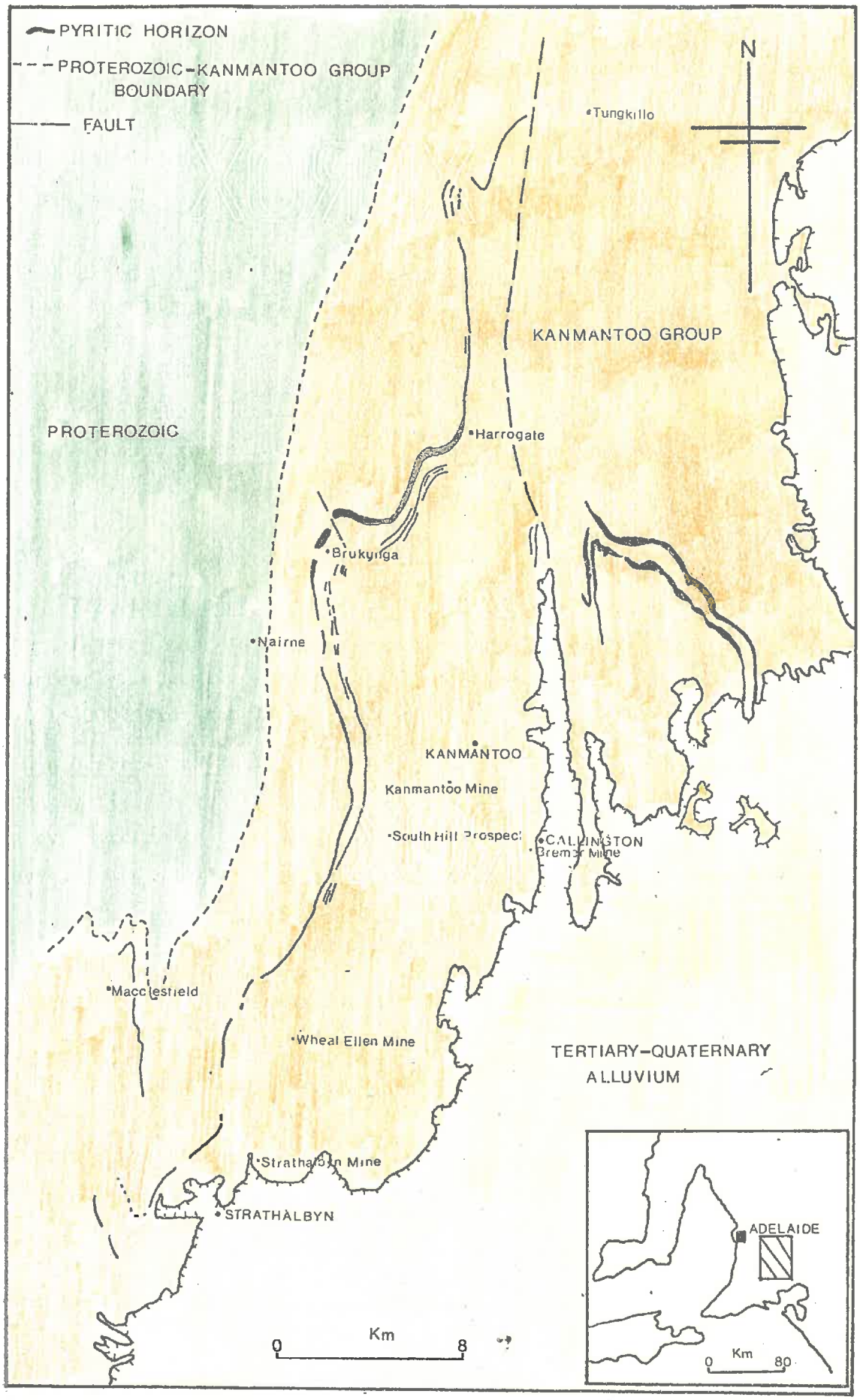

FIG. 1

LOCALITY MAP

TABLE 2 STRUCTURAL NOMENCLATURE

Deformations	Surface	Lineation	Fold
Initial Structures	So - Bedding		
D1	S_1 - slaty cleavage and schistosity	L_1 - Lineation in S_1 due to elongation of biotite, muscovite and andalusite	F_1 - small folds and mesoscopic folds in So
D2	S_2 - axial plane of east-west crenulation, crenulation cleavage	L_2 - fold axis of crenulation	F_2 - crenulation in S_1
D3	S_3 - axial plane of north-south crenulation, crenulation cleavage	L_3 - fold axis of crenulation	F_3 - crenulations in S_1
D4	S_4 - axial plane of late stage kinks in S_1. Minor faults and cross-cutting veins.		

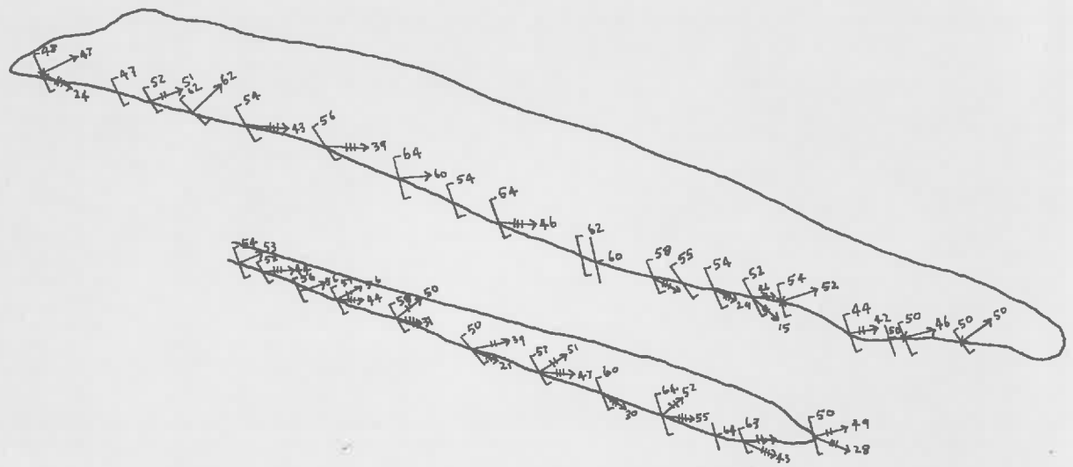

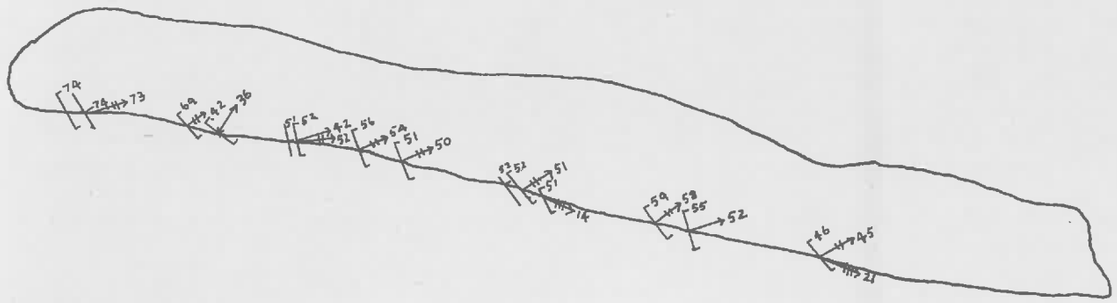

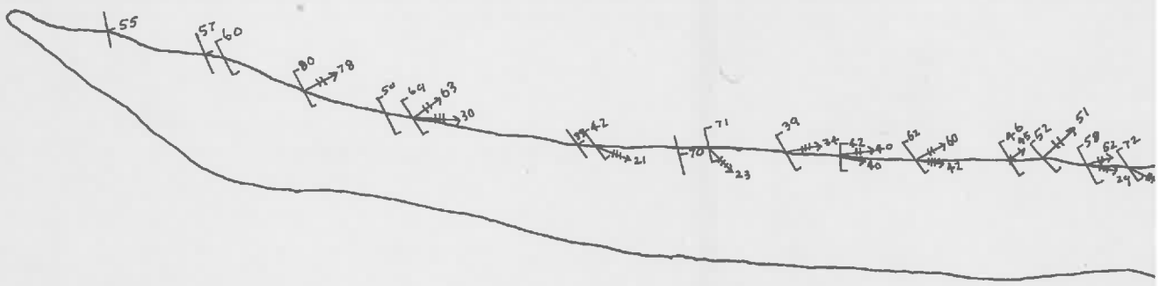

SOUTH HILL PROSPECT: HIGHWAY CUTTINGS
STRUCTURAL DATA
LEGEND

- BEDDING S_0
- SCHISTOSITY S_1
- S_0-S_1 INTERSECTION
- MINERAL LINEATION L_1
- CRENULATION LINEATION L_2
- CRENULATION LINEATION L_3
- HIGHWAY CUTTING

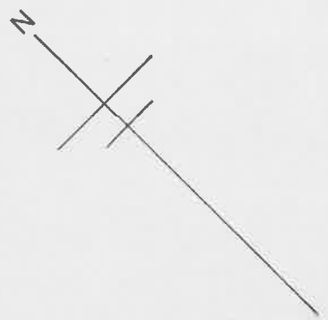

SCALE 1:2400

FIG.4

SOUTH HILL PROSPECT

STRUCTURAL DATA

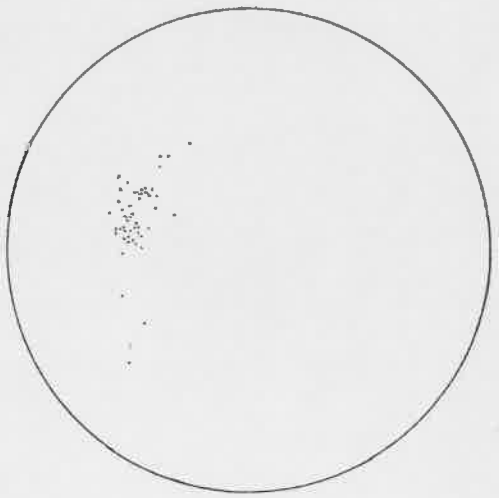

POLES TO S_0

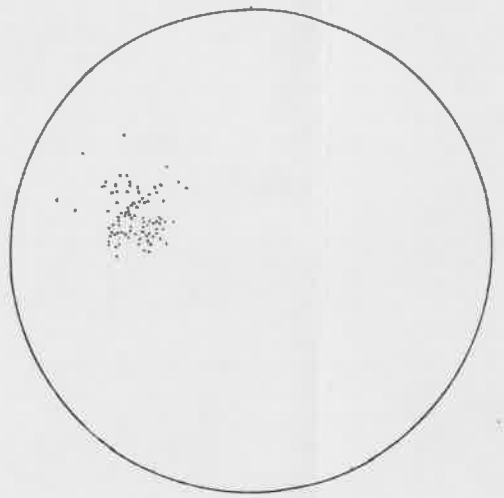

POLES TO S_1

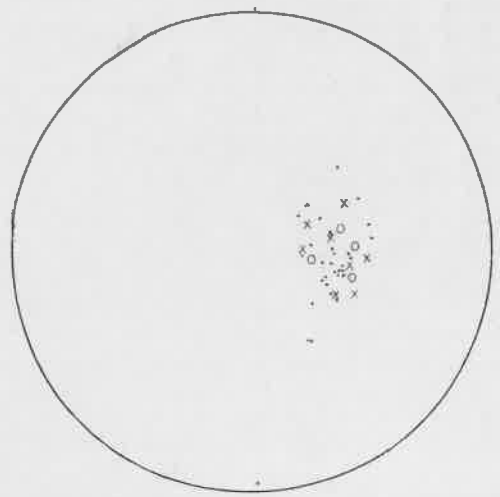

S_0–S_1 INTERSECTION & MINERAL LINEATION L_1 x

FOLD AXES F. o

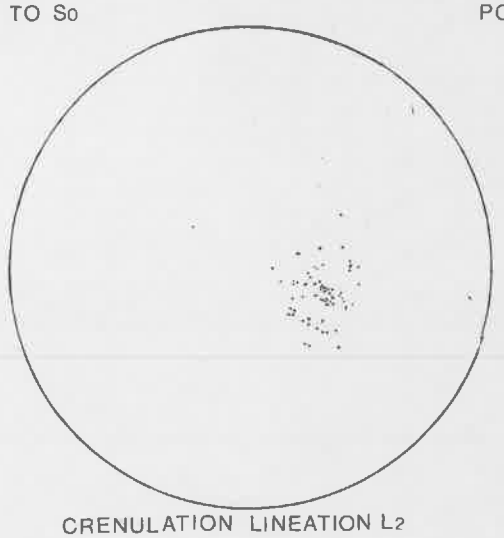

CRENULATION LINEATION L_2

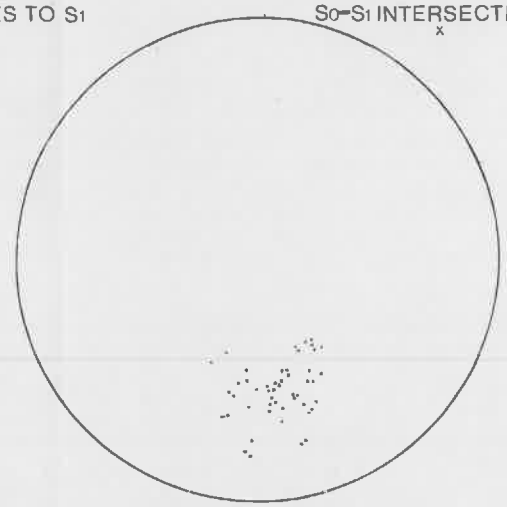

CRENULATION LINEATION L_3

WHEAL ELLEN

STRUCTURAL DATA

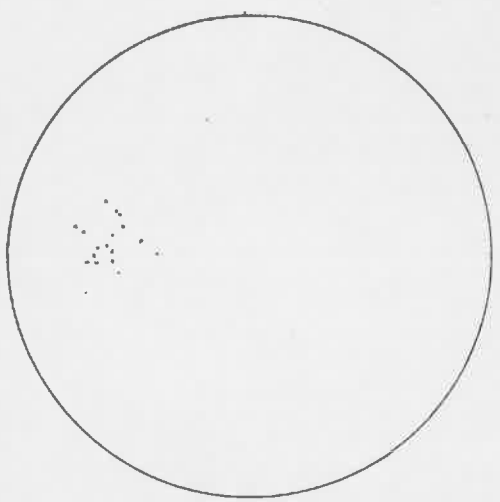

POLES TO S_0

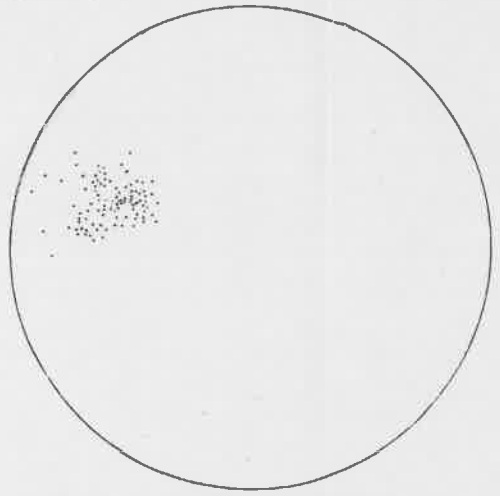

POLES TO S_1

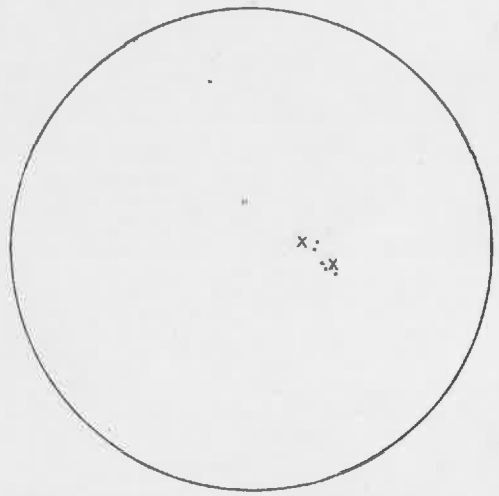

S_0–S_1 INTERSECTION & MINERAL LINEATION L_1

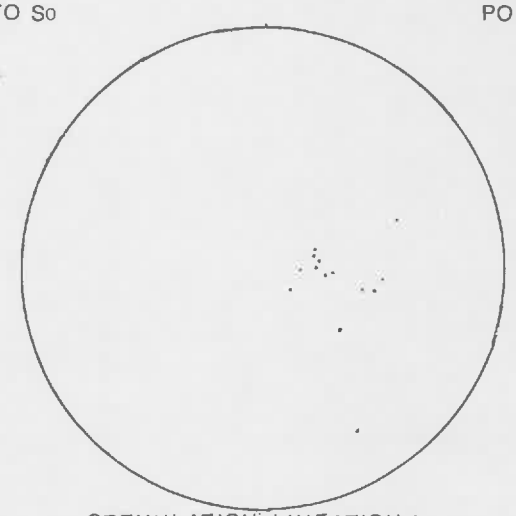

CRENULATION LINEATION L_2

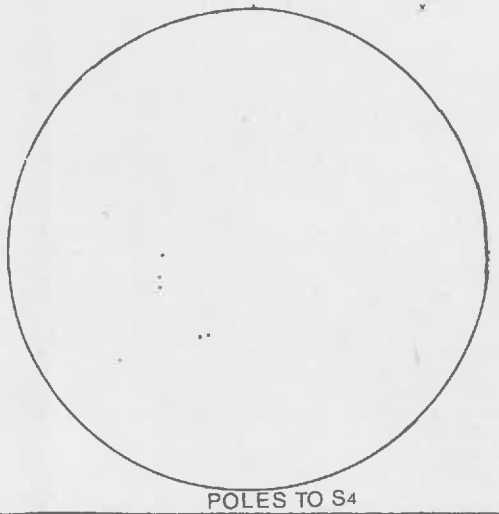

POLES TO S_4

FIG.5

SPRY 1976

PLATE 1

a) Interlayered andalusite and biotite schists parallel to fine scale bedding (So). (Wheal Ellen)

b) Quartz veins concordant to S1 exhibiting pinch and swell structures. (South Hill)

c) Crenulation lineation (L2) in S1, in biotite schist. (South Hill)

d) Pseudo pebbles or subtended sandy layers elongate parallel to S1 in quartz-mica schist. (Wheal Ellen)

e) Interlacing kink surfaces in quartz-mica schist. (Wheal Ellen)

a

b

c

d

e

by Poole (1969) near the South Hill area. They are generally asymmetric and appear to form an interlacing set, (see Fig 1e). These are not conjugate sets because the sense of movement across the kinks is always upper half toward the east. The kink planes lie at low angles and are variable in orientation, (see Fig. 5).

3.9 Evidence for a Deformation Event Prior to F1

Poole (1969) first proposed the possibility of a deformation episode prior to F1 as defined by a pervasive axial plane schistosity S1. He discussed the plunge variations of F1 fold axes and the presence of mullions, possibly produced by an earlier deformation. Poole (op. cit.), concluded that the plunge variations were due to folding of an initially inhomogeneous surface and that the mullions were "most likely to be slivers of rock which have not responded to folding in the same way as the rest of the rock."

Supporting evidence for a possible earlier deformation is provided by inclusion trails in andalusites. The andalusites appear to be pre-F1 because S1 wraps around them (Offler and Fleming, 1968; Spry, 1969, 1972; Misch, 1971). Within these andalusites are elongate biotite, muscovite and quartz which form a trail (Si) that does not continue into the external schistosity (Se) (see Plate 2a). This implies that the inclusion trail is a preserved helicitic schistosity which is older than Se (S1).

An alternative explanation could be that the inclusion trail was part of the S1 fabric and that the andalusite was syntectonic being rotated during the same deformation that produced the S1 surface. The wrapping of the external schistosity around the andalusite could be a result of a shortening process perpendicular to the schistosity direction (Zwart, 1960). The inclusions within the andalusite are smaller than the external micas and quartz, however, the micas constituting S1 have re-crystallized mimetically. The presence of the surrounding porphyroblast may protect the internal fabric from recrystallization. These features are observed in thin section 501/067 (see Appendix 5). There are two reasons for suggesting the second mechanism. Firstly, there are syntectonic andalusites with inclusion trails continuing into S1 (see Fig. 2b) and secondly, these pretectonic andalusites commonly have one end partially enclosed by S1 while the other end is truncated by S1, (see Figs. 2a).

These "pre S1" inclusion trails have been observed in andalusites from Wheal Ellen and South Hill. The presence of these andalusites raises the question of the origin of Poole's (1969) rock slivers. They

PLATE 2

a) Quartz-muscovite biotite inclusion trail in pre S1 (?) andalusite porphyroblast. Inclusion trail is discordant to S1 produced by quartz-fibrolite and may be older than S1. Note, one end S1 partially encloses the porphyroblast whereas other end is truncated by S1 (right end). (crossed polars; x 40; thin section T.S. 501/067)

b) Syn-S1, andalusite porphyroblast with curved internal fabric. Internal fabric continuous with external groundmass S1 schistosity. Note, post-S1 overgrowth on right end of porphyroblast. (crossed polars; x 25; T.S. 501/069)

c) Andalusite with two cores (pre-S1) containing fine grained biotite, quartz and plagioclase (?) surrounded by post-S1 andalusite overgrowth. Note, S1 produced by quartz, muscovite and biotite. (crossed polars; x 25; T.S. 501/069)

a

b

c

may be mullions, and if so would suggest an earlier schistosity.

3.10 F1 Folds

The F1 folds are preserved in four of the observed lithologies. On a scale of 1 cm wavelength, quartz veins produced by metamorphic segregation are isoclinally folded while on a wavelength of 30 cm, isoclinal folds are produced within the andalusite and biotite schists. The pyritic schist on the eastern side of South Hill contain tight macroscopic folds with wavelengths of about 20 m. The fold axis is in approximately the same orientation as the So - S1 intersection and the mineral lineation within S1.

3.11 Discussion of F2 and F3 crenulations

From the plots of all crenulation lineations two clear sets are developed (termed L2 and L3). They occur together in the road cuttings at South Hill where the crenulations with a mean orientation of 35° to 170° appear to overprint the crenulation of orientation 58° to 109°. Marlow (1975) stated that each set of crenulations in the Strathalbyn Anticline has been observed to overprint the other and concluded that the two sets developed during the same deformational period. Difference in style and the observation of one overprinting pattern are the reasons for suggesting the existence of two separate deformations. Mancktelow (pers. comm.) has observed that the orientation of the N-S crenulation is constant whereas that of the E-W crenulation varies and has suggested that this is evidence for the crenulations possibly resulting from separate deformations.

A drawback to the suggested ordering of the crenulations is that the "latter" one has folds associated with it on a macroscale whereas the earlier one does not. In general it has been found that the size of folds decreases during successive deformations.

4. METAMORPHISM

4.1 Introduction

This section summarises the petrology of the main rock types, their response to metamorphism, the most important mineral assemblages, estimation of P-T conditions of metamorphism and the time relationship of crystal growth with respect to deformation.

4.2 Petrology

4.2.1 Quartz-mica schist

Quartz and biotite grains display a preferred orientation which manifests S1. Individual grains are approximately 0.3 mm in length and are strain free; composite grains are larger with the aggregate showing undulose extinction. Quartz-quartz boundaries are generally straight and triple point junctions are common.

Biotite is pleochroic ranging from straw to red-brown. It is generally located along quartz grains boundaries; grains are up to 1 mm in length. The presence in the biotites of minor amounts of monazite or zircon are indicated by the surrounding pleochroic haloes. Muscovite is less common than biotite; most of it is later than the biotite as it cross-cuts the main schistosity.

Plagioclase is slightly coarser and more equidimensional than quartz. Maximum extinction angles of albite twins indicate compositions from An_{10} to An_{22}.

Garnet occurs as rare, scattered colourless idioblasts ranging up to 0.5 mm in diameter. Apatite and zircon are common accessory minerals.

4.2.2 Biotite Schist

Biotite schist differs from quartz-mica schist only in the greater abundance of biotite and muscovite, both of which are parallel to S1. Colourless chlorite which is a breakdown produce of biotite occurs as subhedral flakes cross-cutting S1. Minor andalusite, fibrolite, staurolite and garnet are also observed; their relationship to the matrix will be discussed in the following section.

4.2.3 Andalusite Schist

This unit is petrologically very important as it provides evidence for the grade of metamorphism and for the relationships between metamorphism and deformation. The peak of metamorphism appears to have been associated with F1.

Biotite, muscovite, plagioclase and quartz characteristics are the same as those of the first rock types described above.

There is evidence for the growth of syntectonic andalusites as well

as pre-tectonic andalusites (see Section 3.9). For the syntectonic type the quartz-mica matrix, parallel to S1, continues into the porphyroblast and forms a helicitic trail (see Plate 2b). It is possible that these crystals grew on the locus of a later crenulation in which case they would be post-tectonic to S1. However, the sense of rotation is constant for each andalusite exhibiting the rotated trail. Absence of a crenulation in some thin sections showing the trail supports a syntectonic origin. Syntectonic andalusites are found at Wheal Ellen, South Hill and have also been reported in the Strathalbyn Anticline (Marlow, 1975).

Two stage growth including post-tectonic development is indicated by zoned andalusites with cores containing fine grained quartz, biotite and possibly feldspar surrounded by inclusion free andalusite. Any inclusion trail existing in the latter wraps around the inclusion bearing cores but preserves Se (S1). This suggests the areas of inclusions are older, possibly pre-tectonic, and the "inclusion-free" area is post-tectonic.

Andalusite commonly has a rim of muscovite and quartz which may have been produced from the following reaction:

$$\text{andalusite} + k^{+} + H_2O \rightleftarrows \text{muscovite} + \text{quartz}$$

A modification of this is observed where Fe-oxides and a coarser pleochroic yellow-brown to green-brown biotite occurs in the rim. This biotite (probably low in Fe^{3+} and Ti^{2+}) is discordant to S1 manifested by the fine grained red-brown biotite which may be high in Fe^{3+} and Ti^{2+}. The following reaction is a possibility:

$$\text{andalusite} + \underset{(\text{high } Fe^{3+},\ Ti^{2+})}{\text{Brown Biotite}} + k^{+} + H_2O \rightleftarrows \text{muscovite} + \text{quartz} + \underset{(\text{low } Fe^{3+},\ Ti^{2+})}{\text{Green Biotite}} + \text{Fe oxides.}$$

The close association of fibrolite with andalusite suggests that the production of fibrolite is merely the result of the dimorphic inversion of andalusite to fibrolite; however, a thorough examination of the fibrolite distribution suggests that two other processes may be responsible for its formation. Two common textures are observed:

1. Fibrolite occurs as mats within recrystallized quartz grains. These grains are surrounded by biotite flakes which are in contact with andalusite filled with quartz inclusions. The distance between fibrolite and andalusite is less than 1 mm but they are not in contact.
2. Fibrolite is intergrown with biotite parallel to S1. The andalusite is in close proximity but is separated from direct contact by quartz and muscovite. Some muscovite is post-S1 but the rest is

intergrown with biotite. The biotite has andalusite inclusions.

Fleming (1971) suggested that andalusite did not invert to fibrolite but formed by microsubsystems as proposed by Carmicheal (1969). The observation of fibrolite at South Hill is consistent with the interpretation of Fleming (op. cit.) The two microsubsystems for 1. and 2. are respectively:

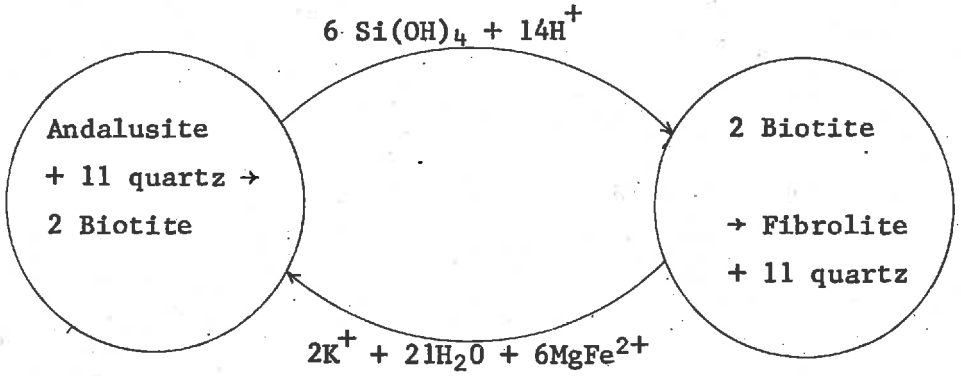

i.e. Andalusite $\rightleftarrows$ Fibrolite

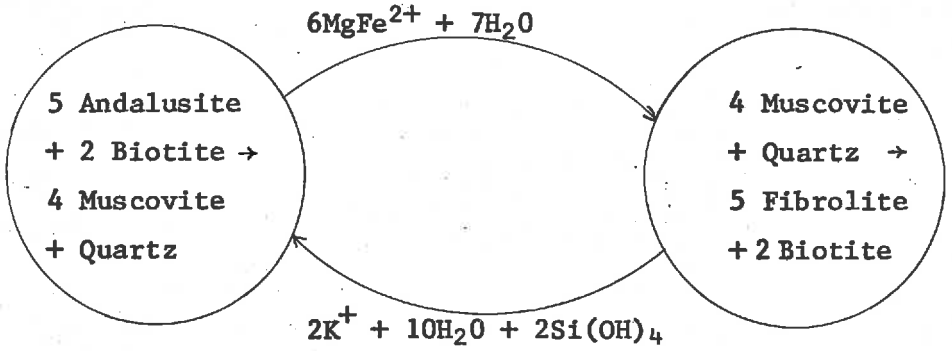

i.e. Andalusite $\rightleftarrows$ Fibrolite

Staurolite either exists as large subhedral crystals or as small fractured grains elongated parallel to S1. In the latter case, there is commonly a direct association between andalusite and staurolite which occurs as a concentration commonly sweeping around the andalusite. Staurolite is intergrown with muscovite and quartz and may be a result of the reaction (Hoschek, 1968):

Andalusite + Biotite + H_2O $\rightleftarrows$ Staurolite + Muscovite + Quartz

Two different forms of chlorite occur. The most common is a late stage coarse variety with a very pale green tint. It is later than staurolite and is often associated with muscovite and almandine garnet (electron-probe work of Lindqvist (1969) suggests that the garnets are almandine). Two reactions may be responsible for these associations:

1. Staurolite + Biotite + Quartz + H_2O $\rightleftarrows$ Chlorite + muscovite + fe opaques.
(Hoschek, 1967; 1969).

PLATE 3

a) Inclusion filled cordierite (Cd) (pre-S1 ?) intergrowth with quartz and gedrite (Ge). Subhedral almandine (G) grows in both cordierite and gedrite. (crossed polars; x 25; T.S. 501/101). (Wheal Ellen)

b) S2 crenulation produced by muscovite in S1. Note, the recrystallized muscovite as indicated by polygonal apices. S1 is defined by a quartz-muscovite intergrowth. (plane polarised light; x 25; T.S. 501/011) (South Hill)

c) Post S1 subhedral staurolite (St) wrapping around andalusite porphyroblasts (A). Note, andalusite breaks down to muscovite (Ms). (plane polarised light; x 25; T.S. 501/018) (Wheal Ellen)

d) Chalcopyrite layer (opaques) in Fe rich silicate layer produced by almandine (G), staurolite (St) and biotite (Bi). Note, the quartz and biotite defining S1 is parallel to the sulphide and Fe-silicate layers which probably define So. (plane polarised light; x 25; polished T.S. 501/134) (Kanmantoo Area drill hole KS 104)

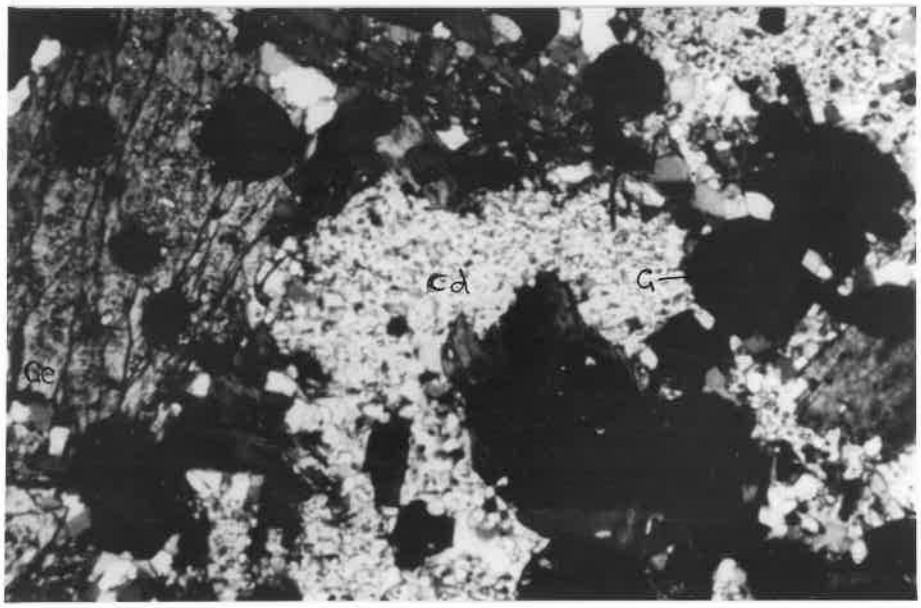

a

b

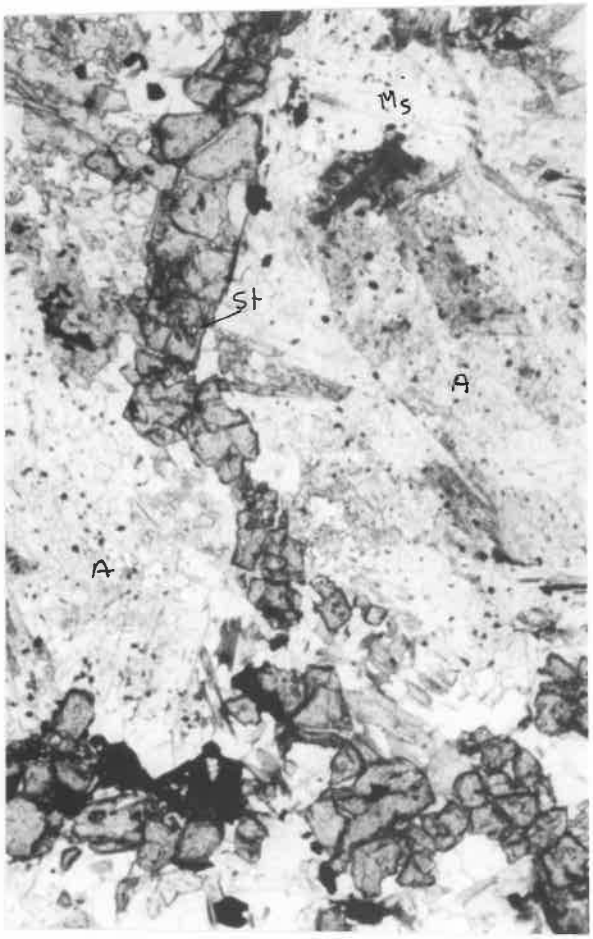

c

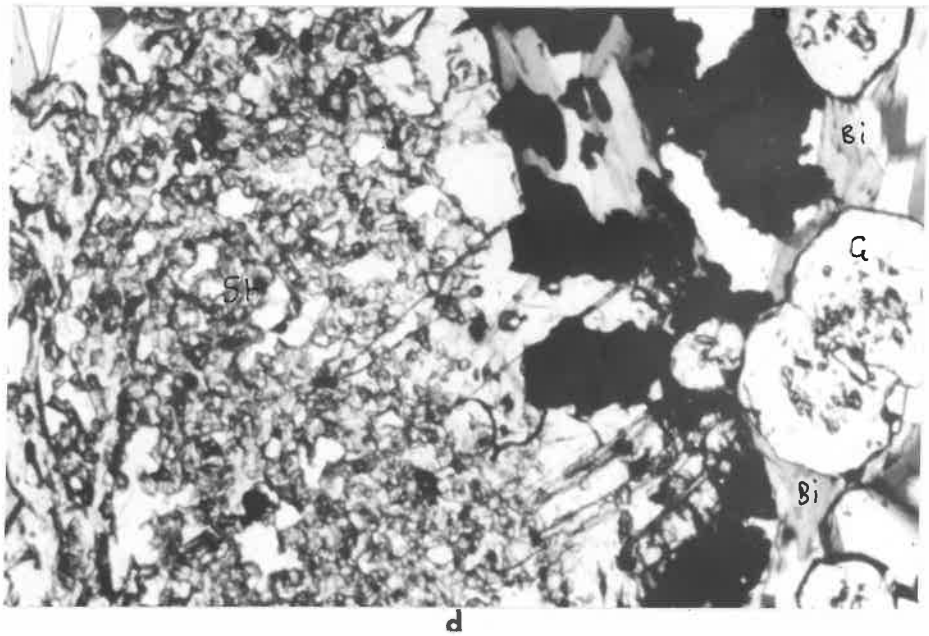

d

2. Staurolite + Biotite + Quartz + $H_2O \rightleftarrows$ Chlorite + Muscovite + Almandine. (Winkler, 1974).

The second variety of chlorite (pastel green) is intergrown with biotite parallel to S1. The localization of chlorite in small areas and the presence of biotite inclusions suggests that the chlorite is an alteration product and not a primary syntectonic (S1) growth.

Almandine (colourless and idioblastic) is more abundant and is coarser grained in biotite-staurolite-chlorite rich layers than in quartz-rich layers. It cross cuts all minerals and is post-S1 but pre-S2.

4.2.4 Garnet-chlorite schist

Three specific mineral assemblages are present. Most important is a garnet-chlorite rock in which chlorite has a preferred orientation and the garnets occur as coarse idioblastic porphyroblasts which are fractured and have been partly broken down to sericite and Fe oxides. Hsu (1968) suggested that almandine can be produced by a breakdown of chlorite; this may account for the garnet-chlorite assemblage.

The two other assemblages are:

garnet ± staurolite ± biotite (± chlorite)

garnet ± staurolite ± biotite

4.2.5 Calc-silicate schist

This rock type is characterized by the presence of either diopside or actinolite.

A diopside-actinolite (or hornblende)-garnet rock is present at South Hill. All the minerals except the salmon pink garnet (possibly grossular) are parallel to S1.

One outcrop at Wheal Ellen consists of a gedrite-cordierite-garnet-chlorite-biotite-quartz and minor plagioclase rock. The cordierite contains many quartz inclusions and is coarse, ragged and has no preferred orientation. This relatively high grade mineral probably grew during F1 and is apparently the western most occurence recorded in the Kanmantoo Group.

At Wheal Ellen a gedrite-actinolite-plagioclase-biotite-fibrolite rock also occurs.

4.3 Conclusions

The relationships between chronology and crystallization are summarized in Table 3. There appears to be one metamorphic event that began before the development of S1 and reached a peak during its development.

The P-T conditions are established in Fig. 6 using key minerals and equations described in the text. Alumino-silicate curves of both Newton

(1966, a and b) and Holdaway (1971) have been plotted. Holdaway's curve (op. cit.) is the more recent but Newton's curve (op. cit.) is in better agreement with the data from sphalerite geobarometry (see section 6.3). Due to the coexistence of fibrolite and andalusite the P-T conditions are probably close to the andalusite-sillimanite line. Using Holdaway's curve (op. cit.) these are 500°-620° for a pressure variation of 1.8 to 3.8 kb. Newton's curve (op. cit.) suggest higher temperatures (500° - 640°) and pressures of 1.8 to 3.8 kb.

Fig. 6. Some experimentally determined equilibrium curves relevant to the assessment of P - T conditions in the Kanmantoo Strathalbyn area.

1. Pyrophyllite $\rightleftarrows$ alumino-silicate + quartz + water (Althaus, 1969)
2. Chlorite + muscovite $\rightleftarrows$ staurolite + biotite + quartz + water (Hoschek, 1967).
3. Fe chloritoid + sillimanite $\rightleftarrows$ Fe staurolite + quartz + water (Richardson, 1968).
4. Granite melt (Luth et. al., 1964).
5. Aluninosilicate phase diagram (Holdaway, 1971).
6. Aluminosilicate phase diagram (Newton, 1966 a and b).
7. Staurolite + quartz + muscovite $\rightleftarrows$ aluminium silicate + biotite + water (Hoschek, 1968).

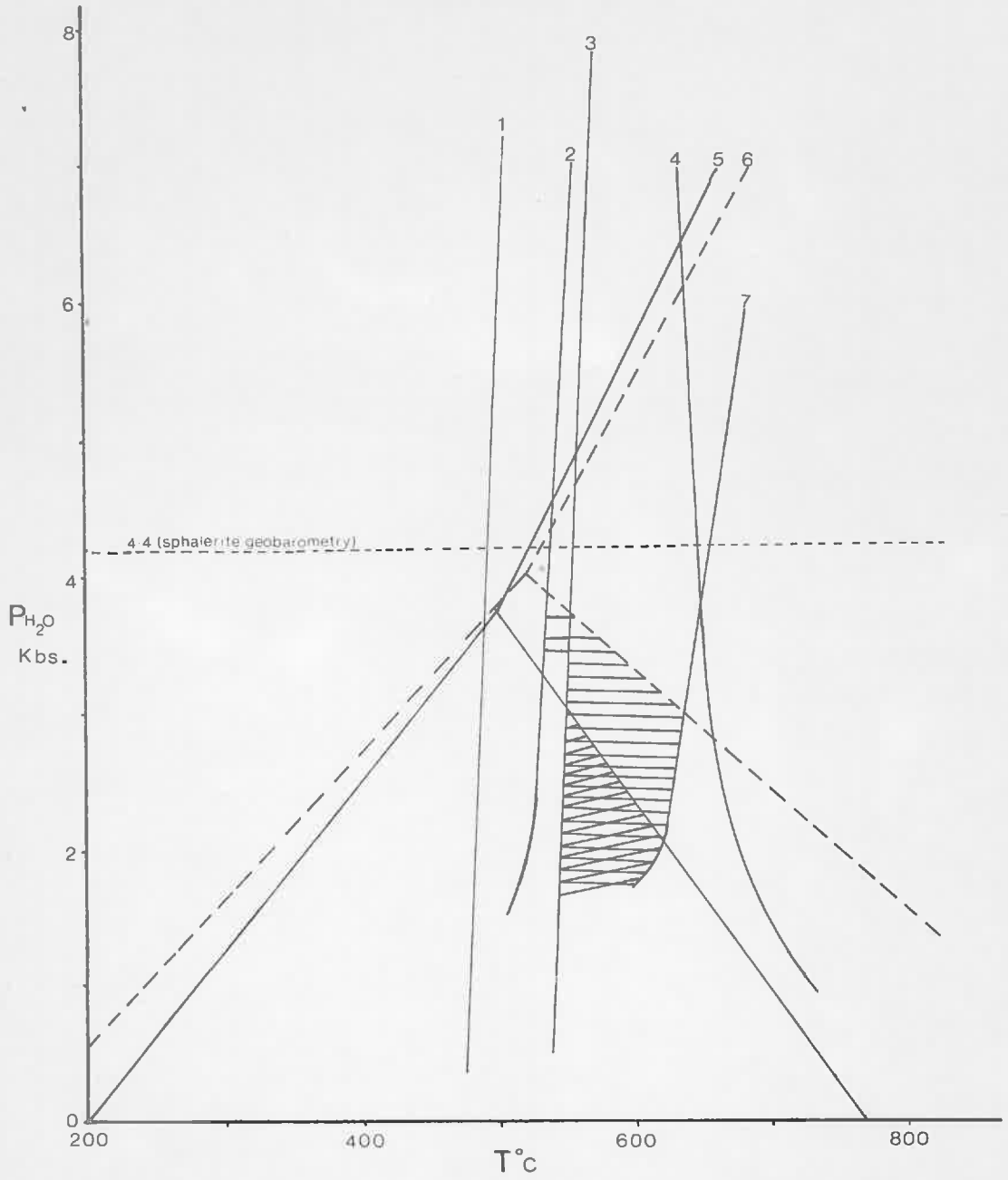

FIG.6 SILICATE STABILITY FIELDS

PS

TABLE 3 CHRONOLOGY OF CRYSTALLIZATION AND DEFORMATION

Phase	Mineral Growth
Pre F_1	Andalusite, Biotite
F_1	Andalusite, Staurolite, Garnet (?), Cordierite (?), Diopside, Hornblende Fibrolite, Biotite, Muscovite, Actinolite
Post F_1	Andalusite, Chlorite, Muscovite, Garnet, Gedrite, Actinolite
S_2	Muscovite, Biotite
Post S_2	Chlorite (?), Muscovite (?), Garnet (?)
S_3	Muscovite, Biotite

5. MINERALIZATION

5.1 Introduction

Sulphide deposits between Kanmantoo and Strathalbyn are of three main varieties, (see Fig. 1). Copper deposits include South Hill Prospect, Kanmantoo and Bremer Mines plus various small scattered deposits near these mines.

Lead-zinc deposits include Wheal Ellen, Aclare, Scott's Creek, Strathalbyn and Glenalbyn Mines.

Pyrite is associated with the Nairne Pyrite Horizon and several other thin pyritic schists occur throughout the Kanmantoo Group.

A detailed study of the mineralization was undertaken at South Hill Prospect and Wheal Ellen and less intensive studies have been carried out on Bremer, Strathalbyn and the Kanmantoo Area.

5.2 Wheal Ellen - Mineralization

Comprehensive reviews of Wheal Ellen were given by Wade and Cochrane (1954) and Askins (1968). The Wheal Ellen Mine was worked for two periods, 1857-1866 and 1906-1911, and Wade and Cochrane (op. cit.) estimated that there were 25,000 tons of gossan ore and 50,000 tons of sulphide ore produced. The overall grade of primary ore was 20% Pb, 25% Zn, 12oz/ton Ag and 3 dwt/ton Au (Askins, 1968).

Exploration drilling was carried out by the South Australian Mines Department between 1919-1920 and in 1954 (Cochrane, 1956). Northern Mining carried out further drilling during the early 1970's.

The dangerous state of the mine made it inaccesible, hence sulphide samples have been obtained from surface dumps and drill holes.

The single orebody has been worked over a length of 230 m, a width of up to 4.3 m and to a depth of 110 m. It has a sheet or tabular shape and is parallel to So and S1, (see Fig. 9).

Within the Middle Air Shaft the ore outcrops as a massive iron rich sandstone. Either side of the orebody the rocks appear to be sheared parallel to S1. The shear zone (2.5 m wide) can also be observed in the Spence Shaft. The surface exposure of the shear zone is indistinguishable from the unsheared country rock. The shear zone probably extends the length of the orebody; there is no field evidence to suggest it extends any further. The following opaque minerals, listed in approximate decreasing order of abundance were observed under the microscope:

(1)	sphalerite	(ZnFe)S
(2)	pyrite and melnikovite-pyrite	FeS_2
(3)	galena	PbS
(4)	chalcopyrite	$CuFeS_2$

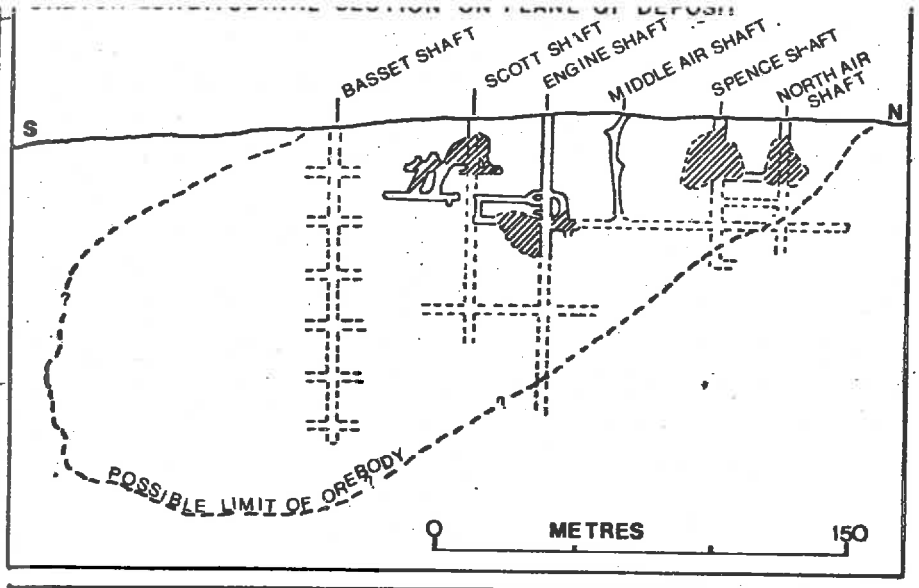

WHEAL ELLEN

MODIFIED AFTER COCHRANE 1958

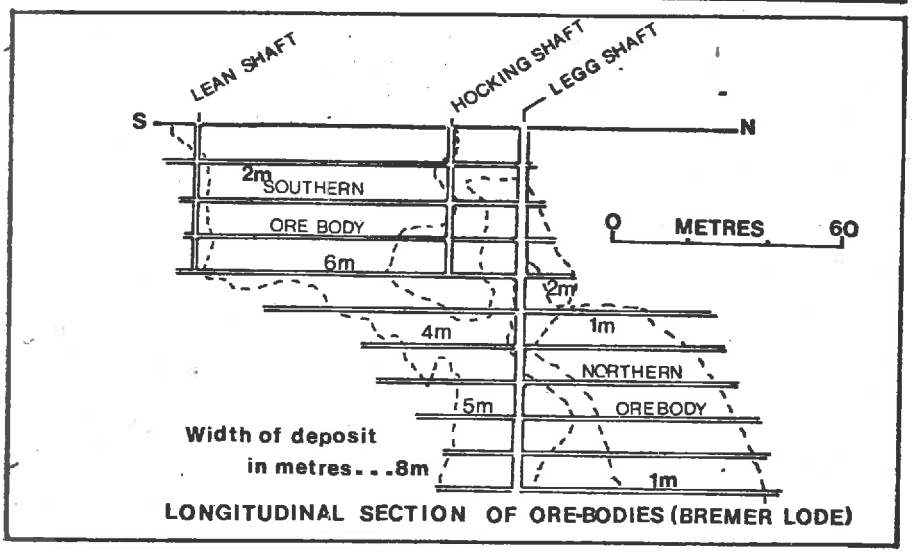

LONGITUDINAL SECTION OF ORE-BODIES (BREMER LODE)

BREMER

MODIFIED AFTER DICKINSON 1942

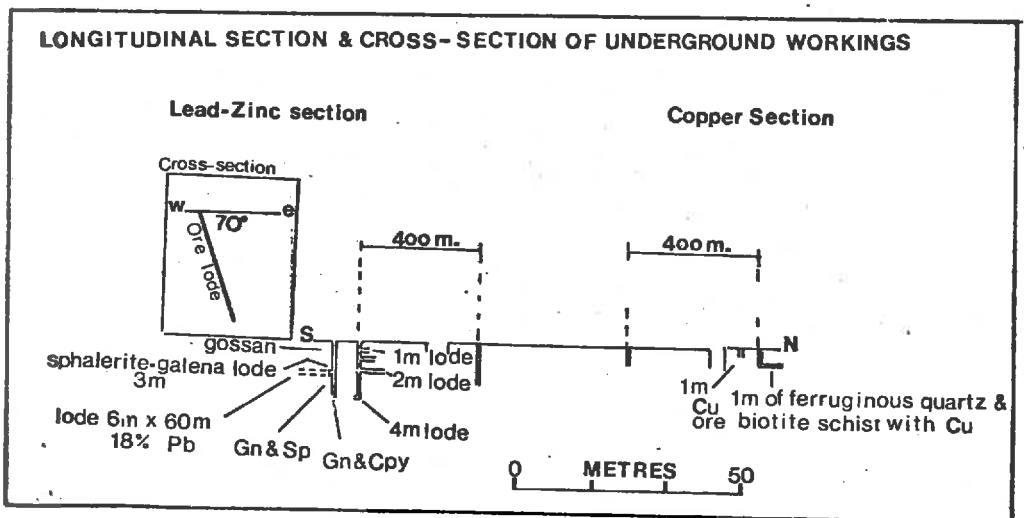

STRATHALBYN

MODIFIED AFTER COCHRANE 1954

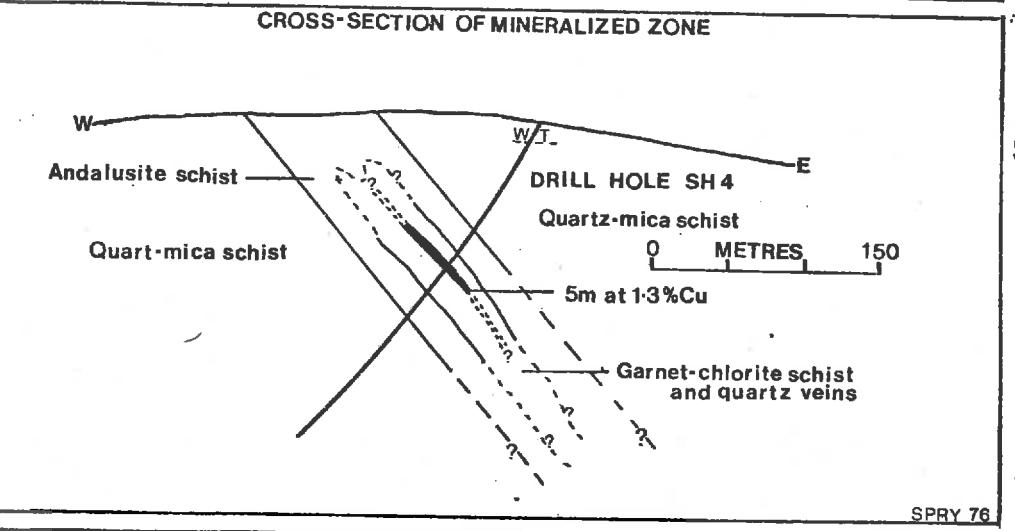

SOUTH HILL PROSPECT

FIG.9 MINE SECTIONS

(5)	gahnite	$ZnAl_2O_4$
(6)	tetrahedrite	$Cu_8Sb_2S_7$
(7)	marcasite	FeS_2
(8)	pyrrhotite	$Fe_{1-x}S$
(9)	boulangerite	$Pb_5Sb_4S_{11}$
(10)	arsenopyrite	FeAsS
(11)	magnetite	Fe_3O_4
(12)	galenobismutite (?)	$PbBi_2S_4$

Mineralization appears to be of two varieties. Massive ore within biotite schist and mineralization within quartz veins both of which parallel So and S1.

The massive ore is a medium to coarse grained intergrowth of pyrite, sphalerite and galena. Sphalerite, up to 1 mm, is the most common sulphide and is intergrown with galena. Triple point junctions indicate recrystallization, however, the most common feature is grains with coarse randomly orientated deformation lamellae. Galena is located in contact with or near euhedra of pyrite grains up to 4 mm in size.

Inclusions of galena, pyrite, pyrrhotite occur within sphalerite grains. The pyrrhotite exists as anhedral to euhedral laths, 0.2 mm in length and also occurs along sphalerite-galena interfaces. Tetrahedrite and chalcopyrite similarly grow on this interface, chalcopyrite having exsolved from sphalerite. Tetrahedrite is more common as wispy inclusions, 0.1 mm in size, within galena. Its distribution and form are suggestive of exsolution bodies, although Ramdohr (1969) suggested that exsolution would be unlikely due to differences between galena and tetrahedrite structures.

Boulangerite occurs as grains up to 1 mm in length, enclosed within galena.

Gahnite is found in both massive and vein ores, the grains are subhedral and up to 1 mm in diameter. It is intergrown with galena and also contains minor inclusions.

A mineral tentatively identified as galenobismutite is present within the massive sulphide ore. This mineral is strongly bireflectant and anisotropic and has a prominent cleavage. It has a Vicker's hardness of 97 to 101 and a reflectance of 24 to 29.

There are some minor compositional differences between the massive ore and the quartz vein mineralization. In the latter arsenopyrite is present, galenobismutite (?) is absent and there is an increase in the pyrite and chalcopyrite content.

In the massive ore, coarse euhedral primary pyrite is more abundant

than minor secondary varieties of pyrite including melnikovite-pyrite and marcasite-pyrite intergrowths whereas in the vein ore secondary varieties are more abundant. Melnikovite-pyrite and marcasite-pyrite intergrowths are most likely to have been produced by a breakdown of pyrrhotite. Porous secondary pyrite with inclusions of gangue, secondary magnetite and ilmenite occur in contact with inclusion-free primary pyrite.

Previously mentioned (2.2) were pyritic schists that occur near the Wheal Ellen and South Hill mineralization. In these schists pyrite, minor chalocopyrite and sphalerite are parallel to S1.

5.2.1 Discussion of Textures

The textures exhibited by the sphalerite, galena and pyrite are typical of a regional metamorphic environment. Pyrite, a mineral of high form energy grows as porphyroblasts while the lower form energy of sphalerite and galena results in the absence of crystal faces (Stanton, 1964; McDonald, 1967; Vokes, 1971). This texture is similar to the Caledonide ores of Norway (Vokes, 1968) and Mt. Isa (McDonald, 1970). Pyrite of lower form energy show "caries" textures.

Veins of galena, sphalerite and chalcopyrite are present in pyrite and arsenopyrite, but the texture is not necessarily due to a difference in time of crystallization but probably reflects a difference in sulphide ductility. Pyrite and arsenopyrite are deformed by brittle fracture whereas galena, sphalerite and chalcopyrite are deformed by ductile flow.

The intergrowth of gahnite, galena and quartz with an absence of sphalerite suggests that gahnite may have formed as a result of sphalerite breakdown. The andalusite is less than two metres from the mineralization as such the gahnite is envisaged to have formed by the following mechanism: (Hobbs, 1975):

$$ZnS + Al_2SiO_5 + O_2 \rightleftarrows ZnAl_2O_4 + SiO_2 + S_2$$

The elongate nature of disseminated sulphides and the metamorphic textures suggest the mineralization is pre or syn F1.

5.3 South Hill Prospect

5.3.1 Introduction

Although there is no record of any production for the South Hill deposit there are three pits which indicate exploratory attempts.

In 1971 Mines Exploration Pty. Ltd. drilled seven holes along the line of mineralization over a distance of 800 metres. The following results obtained indicate the mineralization to be uneconomic:

SH1 - no mineralization	SH5 0.6 m @ 0.28% Cu
SH2 - 3.1 m @ 0.23% Cu	SH6 2.7 m @ 0.23% Cu
SH3 - 4.8 m @ 0.20% Cu	1.5 m @ 0.40% Cu
SH4 - 4.3 m @ 1.23% Cu	SH7 4.8 m @ 0.32% Cu

The mineralization is found in three lithologies, garnet-chlorite-andalusite schist, biotite schist and quartz veins concordant to S1. The sulphide content is greatest in the quartz veins (5.1% Cu is recorded in SH7 290'-291'). Minor disseminations of sulphide up to 2 mm in length are located in the biotite schist. Garnet-chlorite bands within andalusite schist contain sulphides in veinlike bodies parallel to S1. Since S1 and So are both parallel to the mineralized zone it is impossible to determine whether mineralization was related to bedding or was localized in S1 during F1 (see Fig. 9).

5.3.2 Mineralogy and Texture

The following opaque minerals were recognized in polished and polished-thin section and are listed in approximate order of decreasing abundance.

1.	chalcopyrite	$CuFeS_2$
2.	pyrite and melnikovite-pyrite	FeS_2
3.	ilmenite	$FeTiO_3$
4.	chalcocite	Cu_2S
5.	marcasite	FeS_2
6.	magnetite	Fe_3O_4
7.	mackinawite	(Fe,Co,Ni)S
8.	sphalerite	(Zn,Fe)S
9.	pyrrhotite	$Fe_{1-x}S$

The sulphide assemblage consists mainly of chalcopyrite with varieties of primary and secondary pyrite intergrown. Chalcopyrite occurs as massive areas 1 cm in size but mostly as anhedral grains (1 mm). It has been deformed by brittle fracture and ductile deformation. A minor folded chalcopyrite layer resembles folded sulphide observed at Aclare Mine (Askins, 1968) and Mt. Isa (McDonald, 1970). Chalcopyrite is strained and exhibits coarse deformation lamellae.

Mackinawite forms dendrites and fine lamellae through chalcopyrite in two intersecting sets. The individual lamellae are usually less than 0.1 mm long and show a constant orientation through the complexly twinned chalcopyrite. The optical properties are similar to valleriite, however, Lindqvist (1969) analysed similar lamellae at Kanmantoo by electron microprobe and showed them to be mackinawite. Ramdohr (1969) suggested that such lamellae are not due to exsolution but are a breakdown of non-

stoichiometric chalcopyrite.

Pyrrhotite occurs as rounded blebs (<<0.1 mm) within chalcopyrite or secondary pyrite with which it is intergrown.

Sphalerite exists mainly as dendritic inclusions but forms rounded anhedral blebs in chalcopyrite <<0.1 mm diameter. This is clearly an exsolution texture since the sphalerite, in turn, contains very minute inclusions of chalcopyrite.

Primary euhedral pyrite occurs in quartz veins and as needle like grains parallel to S1 in the enclosing schist. The secondary pyrite varieties are the same as observed at Wheal Ellen.

Steel-blue chalcocite forms along fine fractures and as rims around chalcopyrite, probably as a result of supergene oxidation.

Magnetite and ilmenite are distributed throughout the iron-rich silicates. Ilmenite is elongate parallel to S1 and is confined to Fe and Ti rich red-brown biotites. Fe and Ti may have been released from biotite during the early stages of F1 resulting in ilmenite formation. Magnetite is located as anhedral grains within biotite, chlorite, almandine, staurolite and andalusite.

5.3.3 Silicate-Sulphide Relationships

The problem of whether the mineralization is related to So or to remobilization and concentration in S1 cannot be resolved on a macroscale here, and microscopic evidence must be used.

A feature of part of the South Hill mineralization is the elongate nature of sulphides within Fe-silicate bands parallel to S1. The silicates include staurolite, almandine, biotite and chlorite. The association could reflect original Fe rich sediments or alternatively the sulphide could have been introduced during F1 with subsequent breakdown resulting in the release of Fe and the production of post-F1 iron-silicates. The former alternative is more probable for the following reasons. Firstly, the sulphide appears to be discrete elongate grains and not a veinlet. Secondly, there are garnet-chlorite layers where sulphides or remnants of sulphide are absent, so that in some places Fe-silicate has formed without the presence of any sulphide.

5.4 Kanmantoo Area

The Kanmantoo orebody consists of approximately 9 million tons of low grade ore averaging 1% Cu. The orebody is comprised of a number of lenses of mineralization flattened parallel to the axial plane schistosity (S1). The maximum horizontal dimensions of the ore body are 120 x 180 m with a depth of at least 450 m (Verwoerd and Cleghorn, 1975). The copper ore contains chalcopyrite, pyrrhotite and magnetite as the major primary

minerals and is located mainly within garnet-andalusite schists.

Since the report of Lindqvist (1969) on the orebody a large number of drill holes within the mine and exploratory holes north and south of the mine have been completed. Samples selected from some of these drill holes will be discussed.

The following opaque minerals have been identified in polished and polished thin sections and are listed in decreasing order of abundance:

1.	chalcopyrite	$CuFeS_2$
2.	pyrite and melnikovite-pyrite	FeS_2
3.	ilmenite	$FeTiO_3$
4.	marcasite	FeS_2
5.	magnetite	Fe_3O_4
6.	pyrrhotite	$Fe_{1-x}S$
7.	cubanite	$CuFe_2S_3$
8.	sphalerite	(Zn,Fe)S
9.	mackinawite	(Fe,Co,Ni)S
10.	supergene Fe minerals - goethite, limonite	($HFeO_2$; $FeO(OH)nH_2O$)
11.	bismuthinite	Bi_2S_3
12.	bismuth	Bi
13.	gold	Au

Sulphides are parallel to the metamorphic layering and to S1 and are associated with garnet-chlorite-andalusite schists and concordant (S1) quartz veins. This is similar to that observed at South Hill and the main Kanmantoo orebody.

The dominant sulphide assemblages are an intergrowth of pyrite and chalcopyrite. Chalcopyrite forms as massive areas and as disseminations parallel to S1. Chalcopyrite is host to the minor sulphide phases. Pyrrhotite occurs as minute anhedral blebs whereas cubanite and sphalerite appear as exsolution lamellae. Cubanite lamellae are up to 0.1 mm wide and 2 mm long. Mackinawite and cubanite lamellae follow the tetragonal crystal lattice of chalcopyrite and the edges of deformation lamellae (see Plate 4a). No explanation is at present apparent for lamellae of mackinawite and cubanite that follow other orientations.

Cubes less than 0.1 mm and needle-like lamellae parallel to S1 are the only varieties of primary pyrite. Secondary varieties persist throughout the chalcopyrite. In polished section secondary pyrite was observed to be concentrated in the cubanite lamellae and is concentrated near fine fractures that cross-cut the chalcopyrite. It is suggested that cubanite and chalcopyrite were in equilibrium and that sulphur-bearing solutions entered

PLATE 4

a) Cubanite (Cb) and mackinawite (Mk) lamellae in a chalcopyrite (Cpy) host. Note, the lamellae define the tetragonal crystal lattice of chalcopyrite. (reflected light; x 56; polished section (P.S.) 501/050) (Kanmantoo Area)

b) Cubanite (Cb) lamellae in a chalcopyrite (Cpy) host. Note, the confinement of pyrite to the cubanite lamellae and its proximity to the fine fracture. The pyrite probably resulted from sulphur rich solutions entering along the fracture. (reflected light; x 56; P.S. 501/050) (Kanmantoo Area)

c) Intergrowth of cubanite (Cb) and chalcopyrite (Cpy) either as discrete grains or as exsolution lamellae. (reflected light; x 200; P.S. 501/052) (Kanmantoo Area)

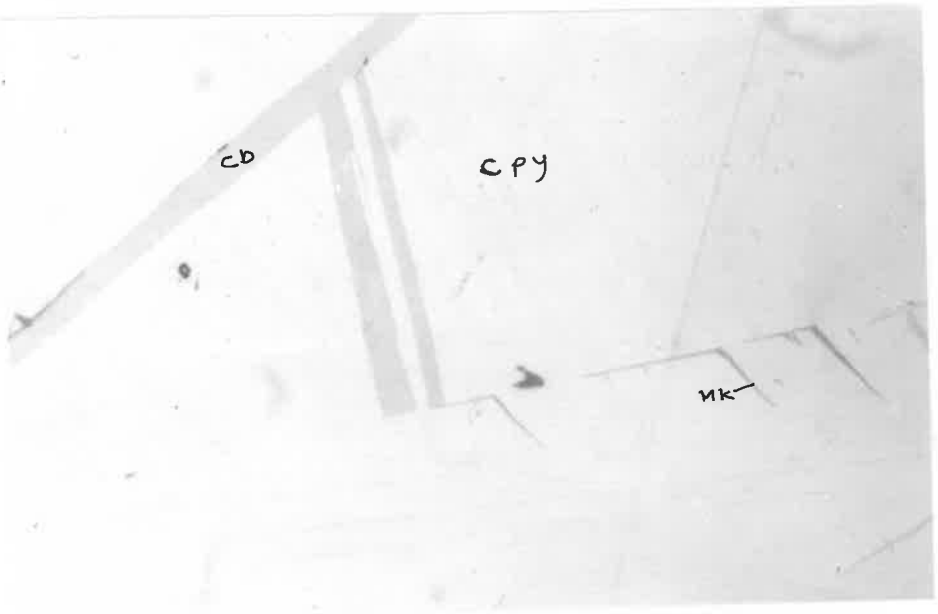

a

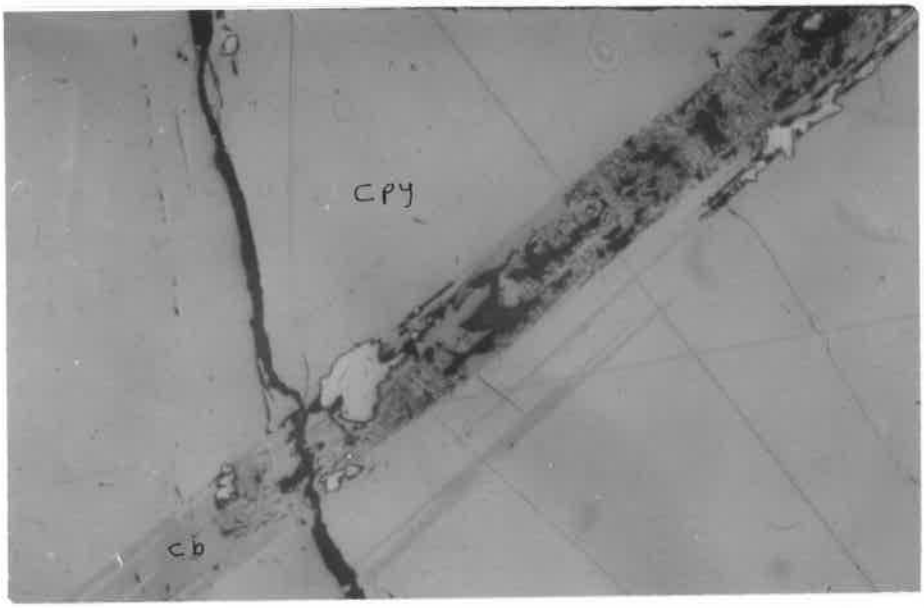

b

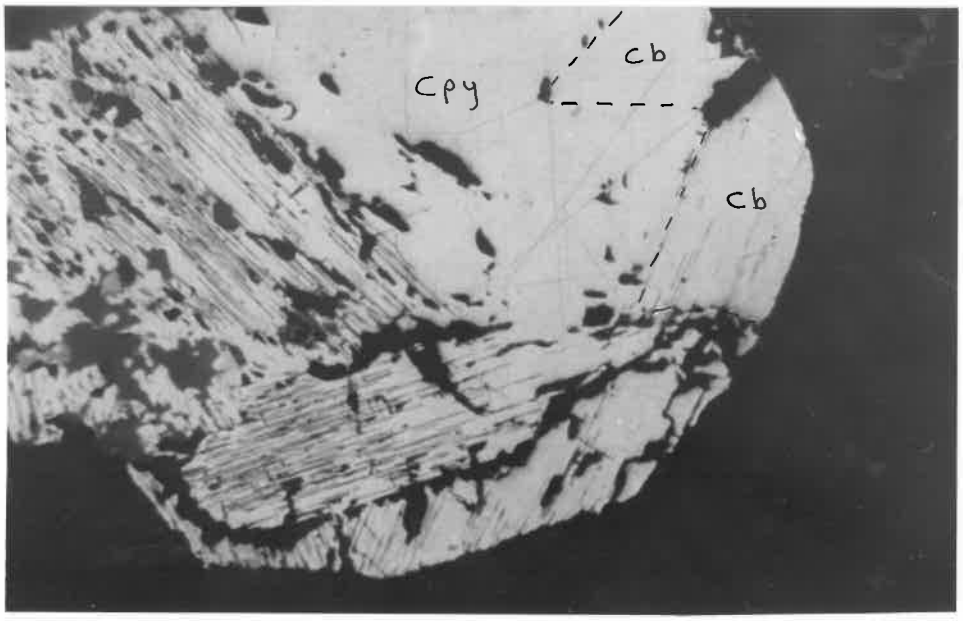

c

along the fractures to produce pyrite in the lamellae (S. Scott pers. comm.) (see Plate 4b).

Traces of gold, bismuth and bismuthinite are observed in chalycopyrite. Bismuth forms cores to bismuthinite rims.

The sulphide together with magnetite and ilmenite have a similar relationship to the silicates indicated at South Hill. Sulphide is intergrown with chlorite, staurolite, biotite and garnet. The staurolite content of these metamorphic layers is greater than those observed at South Hill.

5.5 Bremer Mine

5.5.1 Introduction

The Bremer Mine, on the northern boundary of Callington, was discovered in 1850 and first worked by the Bremer Company. Between 1850 and 1907 there were three periods of working, each period by a different company. Production from the first period yielded about 13,000 tons of copper ore.

Northern Mining leased the area and began drilling in the early 1970's.

5.5.2 Geological Setting

The mineralization is located in biotite schist as veins which form irregular, tabular ore shoots (Duncan, 1973). There are two ore shoots, the Bremer and Boundy lodes averaging 100 m long by 100 m deep by 1 m wide (Dickinson, 1942; Grasso and McManus 1954). The lodes are approximately 90 metres apart, (see Fig. 9).

Duncan (op. cit.) reported that the two mineralized shears are two of a series which traverse the mine area. The mineralized shears strike 140^{o} with a westerly dip varying from vertical to 72^{o}. Outside the mine area a shear zone, striking 200^{o}, cuts the Wheal Pioneer Mine and trends towards the Bremer Mine. The dominant schistosity (S1) has an orientation of 189^{o}. It is suggested the two shear zones, as a result of these orientations, form a complementary shear set related to the F1 folding.

5.5.3 Mineralization

Dump samples indicate that the mineralization is disseminated in biotite schist and as veins associated with quartz. Coarse actinolite surrounds these veins and is probably an alteration product.

Only a brief account of the opaque mineralogy will be given as it is similar to the other mineralized areas mentioned.

Minerals observed in polished section in decreasing order of abundance are:

1.	chalcopyrite	$CuFeS_2$
2.	pyrite	FeS_2
3.	supergene Fe minerals - limonite, goethite	$HFeO_2$; $FeO(OH)nH_2O$
4.	sphalerite	$(ZnFe)S$
5.	ilmenite	$FeTiO_3$
6.	magnetite	Fe_3O_4
7.	mackinawite	$(Fe,Co,Ni)S$
8.	pyrrhotite	$Fe_{1-x}S$
9.	covellite	CuS

In particular, the mineral assemblage is similar to that of the Kanmantoo area but Fe silicates and trace amounts of gold and cubanite are absent. Austin (1863) reported bornite and arsenopyrite while Northern Mining have detected bismuth and bismuthinite in the orebody.

The dominant sulphide assemblage is chalcopyrite and pyrite which form massive areas in quartz veins and elongate disseminations in the biotite schist.

Chalcopyrite contains exsolution blebs and dendrites of sphalerite which in turn contains minute chalcopyrite.

Trace amounts of pyrrhotite and mackinawite are observed in chalcopyrite; pyrrhotite occurs as anhedral blebs while mackinawite forms dendrites and thin lamellae.

Supergene covellite is concentrated along narrow veinlets in quartz which is enclosed by chalcopyrite.

Primary euhedral pyrite, 0.1 mm in size, and inclusion-free pyrite are enclosed within chalcopyrite whereas secondary pyrite forms in veins cross cutting chalcopyrite.

5.6 Strathalbyn Mine

5.6.1 Introduction

The mine is located about 3 km north of Strathalbyn. A summary of the known information concerning the mine is given by Austin (1863), Jones (1913), Cochrane (1954) and Askins (1968).

Three diggings over a kilometre interval are situated in a quartz gossan lode that has a north-south strike and a dip 70°E. Assays suggest a copper lode at the northern end and a lead-zinc lode at the southern end.

The stratigraphic level of the Strathalbyn Mine relative to the Nairne Pyrite Horizon is similar to that of the Wheal Ellen Mine and South Hill Prospect. They may be related to the same horizon even though no

andalusite schist has been found. The absence of andalusite schist may be due to the lack of outcrop. The host rocks to the mineralization are quartz biotite and biotite schists.

5.6.2 Mineralization

Opaque minerals observed in polished section in decreasing order of abundance are:

1.	pyrite and melnikovite-pyrite	FeS_2
2.	chalcopyrite	$CuFeS_2$
3.	marcasite	FeS_2
4.	arsenopyrite	FeAsS
5.	sphalerite	(ZnFe)S
6.	pyrrhotite	$Fe_{1-x}S$
7.	supergene Fe minerals - goethite and limonite	$HFeO_2$; $FeO(OH).nH_2O$
8.	tetrahedrite	$Cu_8Sb_2S_7$
9.	magnetite	Fe_3O_4
10.	ilmenite	$FeTiO_3$

Pyrite consists of secondary varieties only. Melnikovite-pyrite colloform textures are observed with supergene Fe oxides filling the cracks. Porous inclusion-filled pyrite is intergrown with twinned marcasite.

Ragged anhedral chalcopyrite, anhedral sphalerite (0.1 mm in length) and subhedral to euhedral pyrrhotite is disseminated through pyrite and non-opaque material.

Euhedral arsenopyrite is observed in pyrite but is anhedral within quartz veins where it is replaced by minor amounts of tetrahedrite.

Anhedral secondary magnetite occurs within pyrite while primary euhedral ilmenite is elongate parallel to the dominant schistosity.

The sulphide is mostly located in quartz veins. The orientation of the veins is unknown but it is suggested that it is parallel to S1 (Askins, 1968).

PLATE 5

a) Typical metamorphic texture observed in massive ore (Wheal Ellen). Coarse subhedral pyrite (Py) in an intergrowth of sphalerite (Sp) and galena (Gn). (reflected light; x 56; P.S. 501/110)

b) Pyrite-melnikovite intergrowth. Note, the colloform texture with secondary magnetite (Mg) filling in the fine cracks. (reflected light; x 56; P.S. ST1 207) (Strathalbyn)

c) Galena (Gn)-Sphalerite (Sp) intergrowth with minor galeno-bismutite (?) (Gnb). Note, the fine cleavage in galeno-bismutite (?). (reflected light, x 100; P.S. 501/036) (Wheal Ellen)

d) Fine needles and elongate grains of pyrite (Py) in a quartz-muscovite host. The elongation of pyrite is parallel to S1. (reflected light; x 64; P.S. WE4 360) (Wheal Ellen)

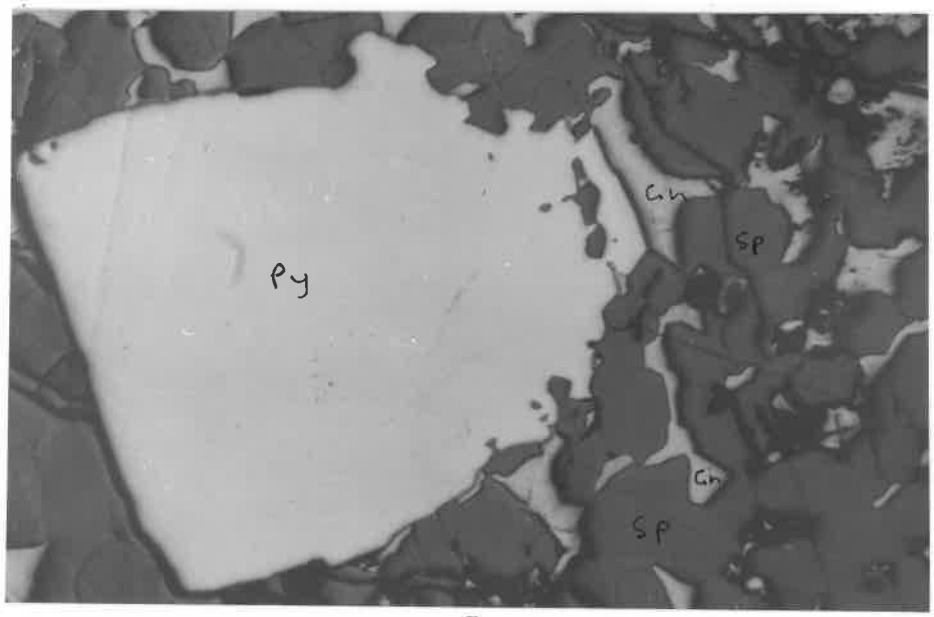

a

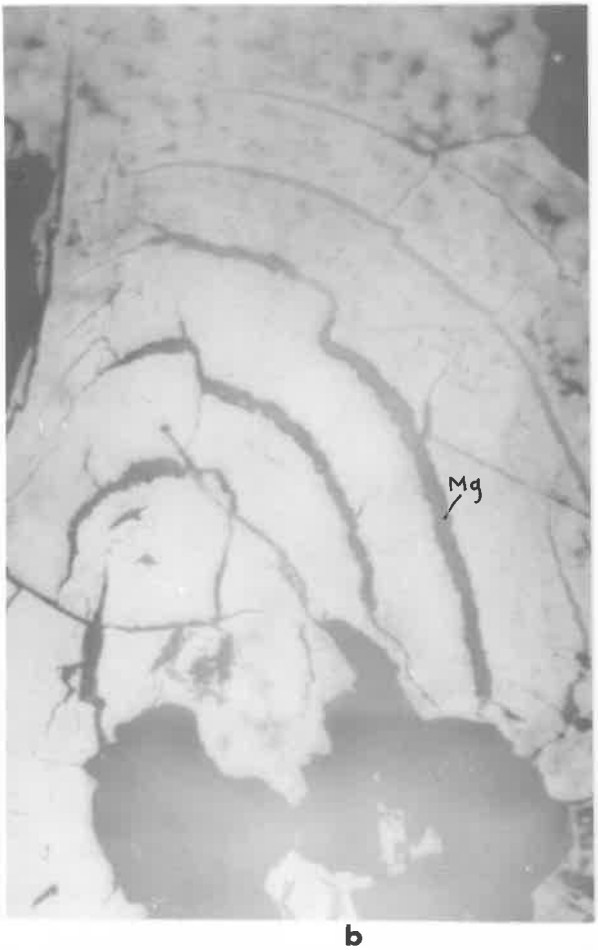

b

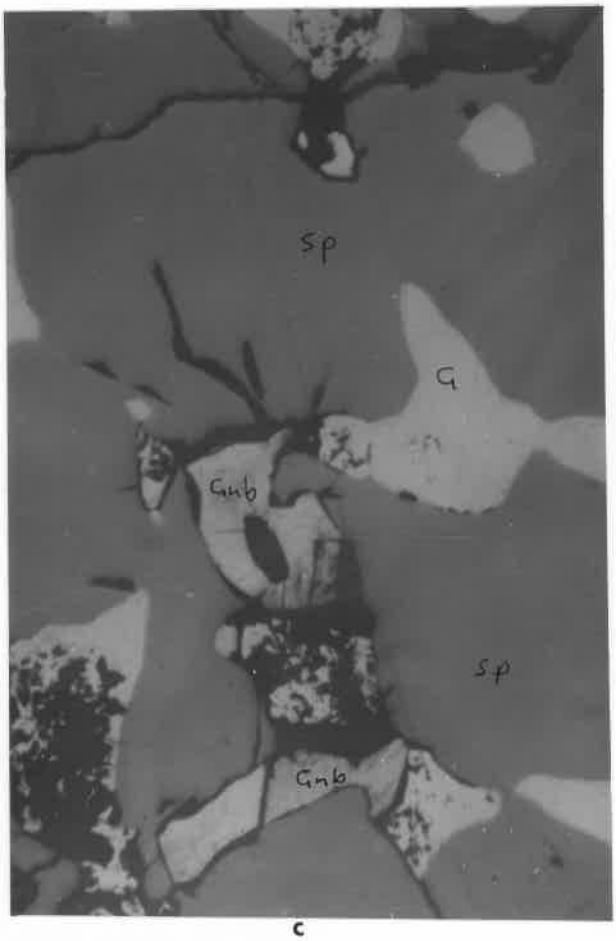

c

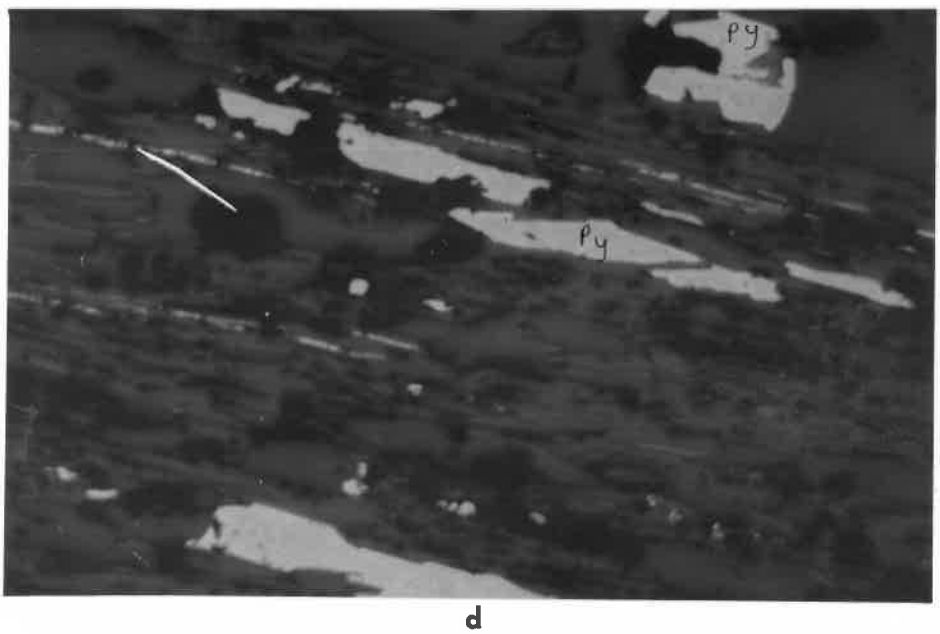

d

6. SPHALERITE GEOBAROMETRY

6.1 Introduction

Scott and Barnes (1967, 1969 and 1971) showed that the constant slope of the sphalerite + pyrite + hexagonal-pyrrhotite solvus can be used as a geobarometer by virtue of the variation in $aFeS$ with pressure along the pyrite + hexagonal-pyrrhotite solvus (Scott, 1973). The Fe content of sphalerite, if in equilibrium with hexagonal pyrrhotite and pyrite, will give an indication of the pressure of metamorphism of sphalerite.

If the sphalerite was in equilibrium with other sulphides during metamorphism, the determination of its pressure might indicate the pressure of metamorphism of sulphide mineralization and possibly the pressure of the associated metamorphic event.

Fifteen samples were analysed by electron probe: seven from Wheal Ellen, two each from South Hill, Bremer and drill hole KS40 (500 m north of the Kanmantoo Mine pit) and one each from drill hole KS123 (2 km north of the Kanmantoo Mine pit) and Strathalbyn. The results can be seen in Appendix 1.

6.2 Discussion

There is a wide variation from 1.1 to 9.0 in the wt.% Fe for all samples, but the variations observed within the Wheal Ellen, South Hill and Bremer samples are small (8.8 to 9.0, 5.7 to 5.9 and 7.9 to 8.1 respectively)(see Appendix 1).

Scott (1973) pointed out that the pyrite, sphalerite and hexagonal pyrrhotite must be in equilibrium for geobarometry to be accurate. This strict requirement is generally only satisfied if they are in direct contact (S. Scott pers. comm.). This was the case for all the Wheal Ellen polished sections, but in the samples for other deposits sphalerite and pyrrhotite existed in trace amounts and generally only as an exsolution product wholly within chalcopyrite. As a result Wheal Ellen is the only deposit for which sphalerite geobarometry is suitable. The dominance of hexagonal pyrrhotite at Kanmantoo (Lindqvist, 1969), which was detected by x-ray diffraction, and at Shephard Hill near Nairne (Skinner, 1958) suggests the pyrrhotite to be mostly hexagonal at Wheal Ellen. This was verified by applying a magnetic colloid to the pyrrhotite from Wheal Ellen and South Hill.

The other main components Zn, S, Cd and Mn were measured because FeS solubility is affected by the presence of such metals as Cd and Mn (Stanton, 1972). Scott and Barnes (1971) showed that the presence of such minor elements do not affect the geobarometer even when several wt.% of

CdS or MnS are present. Bremer samples 501/044 and 501/042 had high Cd values of 0.88% and 2.4% respectively.

The Fe content of sphalerite in Nairne Pyrite samples was measured by Skinner (1958) and the results included in Appendix 1. Skinner (op. cit.) used a wet chemical method for measuring weight % of elements. The average mole percent in sphalerites at Wheal Ellen is 15.2 which is in good agreement with the average value for the two Nairne Pyrite samples of Skinner (op. cit.).

The Shepherd Hill quarry near Nairne is associated with the alumino-silicate assemblage andalusite-kyanite whereas andalusite-fibrolite is the assemblage at Wheal Ellen. Therefore the pressure conditions indicated from the sphalerite geobarometer should be slightly different. However, pressure conditions of 4.4 (±0.5) kb at both places are indicated from the sphalerite geobarometer (see Fig. 7).

The value of 4.4 (±0.5) kb is higher than the range of pressures indicated by Newton (1966, a and b) and Holdaway's (1971) alumino-silicate curves (see Fig. 6). Triple point values are 501°C, 3.76 kb and 538°C 3.95 kb respectively for Holdaway (op. cit.) and Newton (op. cit.). The accuracy of ±0.5 kb obtained from sphalerite geobarometry is just within the andalusite stability field of Newton (op. cit.).

6.3 Conclusion

The presence of sillimanite-kyanite-andalusite within the Kanmantoo Group suggests near-triple point conditions. The value obtained from the sphalerite geobarometer is slightly higher than that indicated by silicate stability fields, 0.7 kb using Newton's (op. cit.) curve and 1.4 kb using Holdaway's (op. cit.) curve.

Scott (pers. comm.) says that sphalerite geobarometry values are commonly higher than silicate values (Lusk, et al., 1975; Lusk, 1976; Groves, et al., 1975, 1976) and may be due to the presence of sub-microscopic Cu in the sphalerite lattice.

In view of the uncertainty involved in the silicate-stability curves and the sphalerite geobarometer the degree of agreement between the two methods is quite reasonable especially when one considers Richardson, et al., (1969) have a triple point of 622°C and 5.5 kb. In this study, the geobarometer probably indicates the pressure of metamorphism.

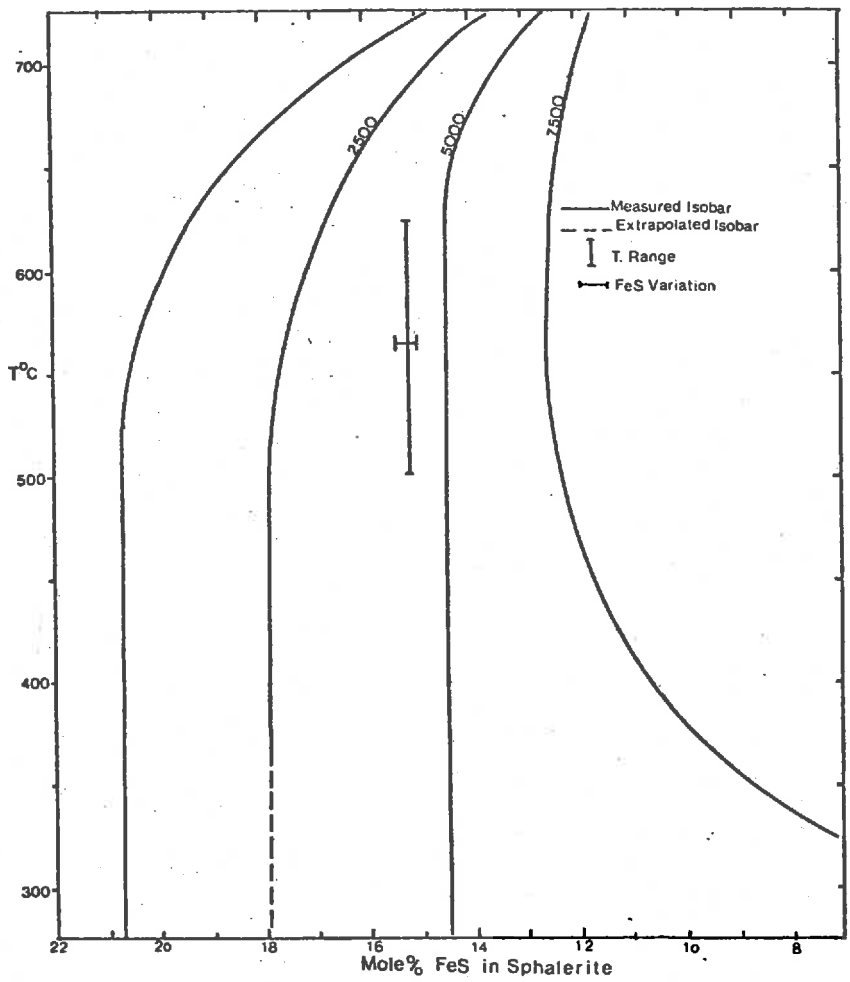

FIG.7 SPHALERITE GEOBAROMETRY : Wheal Ellen (modified from Scott(1971)) P.S.

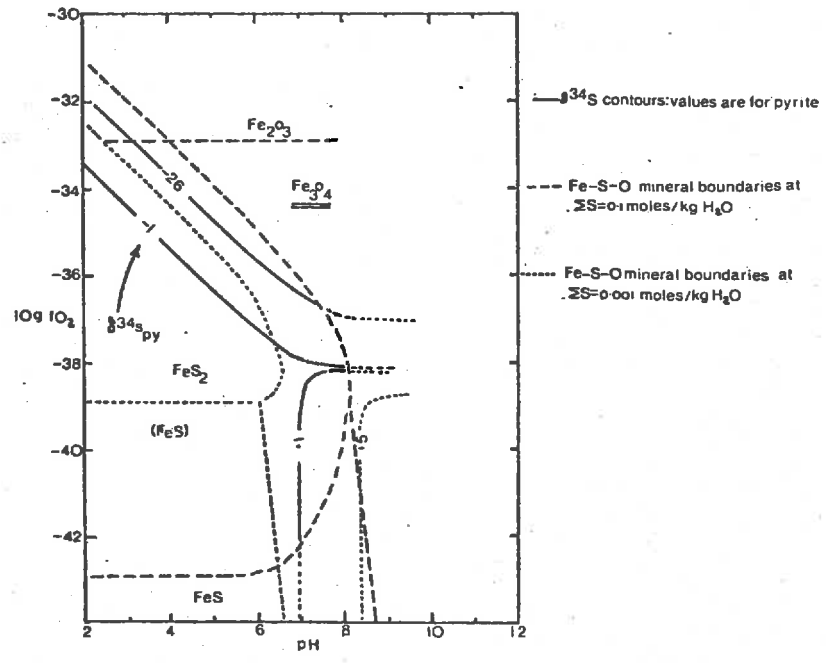

FIG.8 POSITIONS OF $\delta^{34}S$ CONTOURS WITH THE STABILITY FIELDS OF Fe-S-O MINERALS AT 250 °C, $\delta^{34}S_{\Sigma S} = 0$ per mil (modified from Rye & Ohmoto (1974)) PS

7. SULPHUR-ISOTOPE STUDY

7.1 Introduction

A sulphur-isotope study was undertaken on the Wheal Ellen, Strathablyn, Bremer and South Hill deposits, the Nairne Pyrite horizon and samples from drill holes in the Kanmantoo area.

The aim of the work was to determine (1) the source of the sulphur, (2) the mechanisms of deposition and to (3) determine the temperature of sulphide metamorphism and to enable a comparison with silicate stability data.

Previous work in the Kanmantoo Group was carried out by Jensen and Whittle (1969) on the Nairne Pyrite Horizon and by Seccombe and Jones (unpublished data) on the Kanmantoo Mine.

Sulphide species analysed were pyrite, galena, chalcopyrite, pyrrhotite and sphalerite.

7.2 General Considerations

Of the four naturally occuring isotopes of sulphur the two most abundant ^{32}S and ^{34}S are used for sulphur isotope studies. The ratio of ^{34}S to ^{32}S varies depending on physical and chemical conditions including Eh, pH, T and ionic activity of the solutions from which they were derived (Ohmoto, 1972; Rye and Ohmoto, 1974).

Fractionation between coexisting sulphides can be used as a geothermometer because the fractionation factor for the exchange reaction is inversely proportional to the temperature. Fractionations have been determined by a number of workers including Grootenboer and Schwarz (1969), Kajiwara et al. (1969), Kajiwara and Krouse (1971) and Robinson and Ohmoto (1973). All temperature work in this study is based on the data of Kajiwara and Krouse (1971) because they have all the factionation pairs required.

7.3 Geothermometry

The results of the geothermometry studies are summarized on page 25.

The following factors must be taken into account before interpreting the data:

(1) Pyrrhotite and chalcopyrite at Kanmantoo Mine are not in isotopic equilibrium (M. Jones pers. comm.).

(2) Primary and secondary pyrite were measured together for samples that contained both, as they could not be physically separated.

(3) Pyrite has a wide temperature stability field (Rye and Ohmoto, 1974).

(4) The fractionation factor for pyrite-pyrrhotite is small over a large range of temperatures.

Any mineral pairs as a result of the above factors may not be suitable for geothermometry if either is pyrite or pyrrhotite. As a result only the galena-sphalerite pairs from Wheal Ellen are reliable.

			$\Delta\delta^{34}$ S	T°C	Abbreviations
Wheal Ellen	gn-sp	036	1.68	417	po-pyrrhotite
	gn-sp	035	1.66	420	py-pyrite
	py-po	060	1.99	115	sp-sphalerite
	py-po	039	0.09	-	gn-galena
	py-sp	110	0.33	680°	cpy-chalcopyrite
South Hill	py-po	046	5.59	-	
Bremer	cpy-py	042	0.40	788	
Kanmantoo Area	cpy-po	051	0.13	-	

Two sphalerite-galena pairs from Wheal Ellen give temperatures of 417° and 420° (see Appendix 2).

The temperatures, which represent those of sulphide metamorphism are lower than the temperature deduced by silicate stability (see Fig. 6). Sulphides have larger stability fields than silicates therefore the temperature suggests the sulphide has reequilibrated below the metamorphic peak.

7.4 Discussion of Results

The results of the isotope analyses are listed in Appendix 2, and are graphically represented in Fig. 10.

Three slight but distinct categories can be seen clear from Fig. 10. Bremer, South Hill and Strathalbyn all show a similarity in variation. The total range is +3.9 to -4.7 per mil with a mean of +0.1 per mil. Wheal Ellen has a higher mean (+3.4 per mil) and narrow variation (+1.9 to +6.5 per mil) and the Kanmantoo area has the highest mean (+12.5 per mil).

Mineralization at South Hill, Bremer and Strathalbyn lies parallel to S1. Quartz, mica and biotite schists are the host rocks at Bremer and Strathalbyn whereas andalusite schist is the host at South Hill. This implies that the Eh-pH conditions for the ore bearing solutions were similar despite the different wall rock compositions.

The Kanmantoo ore body is not stratiform but related to S1. Results from Seccombe and Jones (unpublished data) give a range of 4.6 to 12.4 per mil. Four samples from drill hole KS104 (0.5 km south of the pit). give values within Seccombe and Jones' (op. cit.) range whereas three samples from KS42 (just north of the pit), give very high values averaging +15.9. Remobilization of mineralization from the main ore body cannot explain this high value since one would expect an enrichment in the higher isotope, ^{32}S, rather than ^{34}S to produce a ratio lower than the

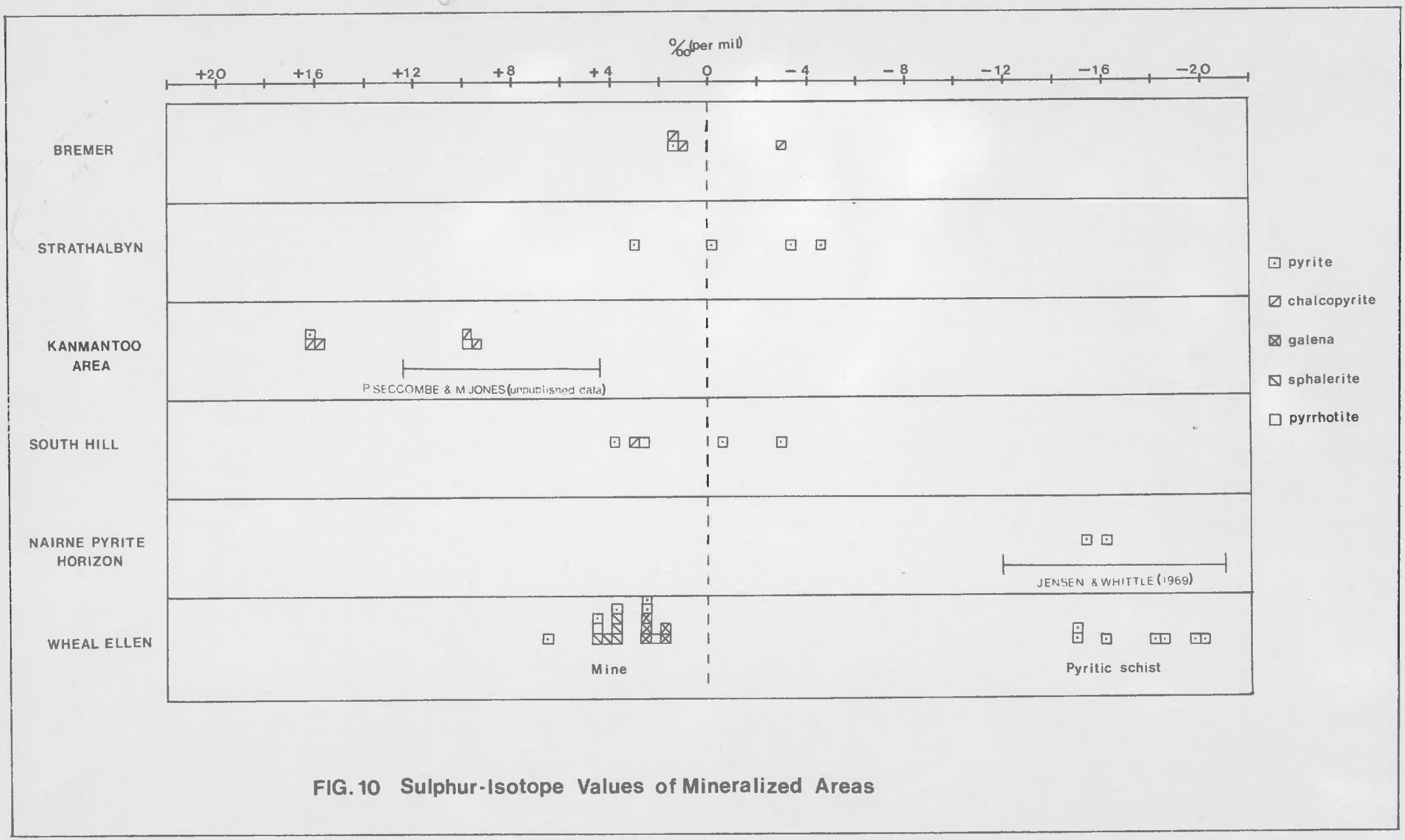

FIG. 10 Sulphur-Isotope Values of Mineralized Areas

main ore body. It may be explained by the ore constituents. Magnetite constitutes about 10% of the Kanmantoo ore body whereas only trace amounts are present in sulphides from drill hole KS42. As magnetite forms in the Kanmantoo ore one would expect a higher fO_2 (Eh) for the ore bearing solutions than for the solutions that produced the mineralized area north of the pit. Hence the lower ^{34}S of the Kanmantoo ore may be due to higher Eh conditions (see Fig. 8). If this argument is correct then it does not explain the average values of +9.9 per mil from drill hole KS104 in which there was also a trace of magnetite.

Variations from -3.1 to +16.2 per mil have been observed between South Hill and the Kanmantoo area less than 2 km away even though the lithologies and mode of formations appear to be the same. This variation almost conforms to the generalizations observed by Stanton and Rafter (1966). The average isotopic composition of sulphur in the deposits they cited is between 0 and +21 per mil, the values for average crustal sulphur (probably mantle sulphur as well) and sulphate in modern sea water respectively. The range (-3.1 to +16.2 per mil) may be due to differential mixing of fluids derived from seas and meteoric waters. This may also explain the variations of KS42 and the Kanmantoo ore body.

This type of mechanism is not unique as similar mixing situations have been reported from Rammelsberg (Anger et al., 1966) and the New Brunswick stratiform massive sulphides (Lusk, 1972).

Seven samples of pyrite from pyritic schists adjacent to the Wheal Ellen deposit were measured to compare with the values from the ore body and the Nairne Pyrite Deposit. The pyritic schists give a mean value of -17.7 per mil and a spread of -15.1 to -20.1 per mil and are comparable to Jensen and Whittle's (1971) values for the mean (-17.2 per mil) and the range (-12.8 to -20.6 per mil) for the Nairne Pyrite Deposit. It appears that, like the Nairne Pyrite Deposit, the sulphide of the pyritic schist is syngenetic and has a bacteriogenic source. Two samples from the Nairne Pyrite Formation, 1.5 km east of South Hill, give values within the range of Jensen and Whittle (op. cit.).

Remobilization of Cu, Pb and Zn from the pyritic schists or even from the Nairne Pyrite Formation in view of the high Pb-Zn and Cu-Pb-Zn (Mirams, 1965) content respectively is a possibility for the source of some of the Kanmantoo Group mineralization. The problem with this possibility is that one would expect an enrichment in ^{32}S to produce a ratio lower than the pyrite horizons and not positive values observed in all of the deposits. Therefore, there does not appear to be any genetic relationship between the mineralization and the pyritic schists as

suggested by Askins (1968).

The trend observed from the ore bodies is for a metamorphic hydrothermal origin and an abiologic sulphur source. The overall variation of -4.7 to +16.2 per mil suggests the ore bearing fluids to be mixtures of source waters, sea and meteoric waters and possibly magmatic which were remobilized during the first deformation. The absence of any magmatic body in the near vicinity of the mineralization suggests magmatic fluids were not a major ore bearing contributor.

8. THE RELATIONSHIP OF THE ANDALUSITE SCHIST TO MINERALIZATION

8.1 Introduction

Lithologies with high base-metal content and associated stratiform ore bodies have been reported in South Australia. The Nairne Pyrite Formation is a series of pyrite-pyrrhotite-bearing greywackes and siltstones in the Kanmantoo Group. Skinner (1958), La Ganza (1959) and George (1967) have shown that it contains a metamorphosed, conformable, sedimentary sulphide deposit. The deposit is high in base metals with values up to 700 ppm Pb, 6200 ppm Zn and 760 ppm Cu (Mirams, 1965).

Jones (1975) and Henley and Brown (1974) have suggested the Ukaparinga schist of Adelaidean age, near Williamstown, which has an average of 3400 ppm Cu to be the source of the syngenetic Ukaparinga copper deposit located in the schist.

The Kanmantoo, South Hill, Wheal Ellen and possibly the Strathalbyn deposits are located within andalusite schist horizons within the Kanmantoo Group. The confinement of copper mineralization for the Kanmantoo and South Hill deposits to the andalusite schist suggests that this lithology might be the source of Cu.

Lindqvist (1969), in attempting to determine the source for mineralization at Kanmantoo, analysed many elements including Cu, Pb, Zn from a series of drill holes intersecting the mineralization and crossing the major lithologies. His results showed that the Cu adjacent to the ore zone was less than 200 ppm and in schists outside the ore zone was around 50 ppm. These values are similar to those of shale (30-150 ppm) quoted by Hawkes and Webb (1962).

As the mineralization is parallel to the axial plane schistosity then, unlike the stratiform Nairne and Ukaparinga deposits the mineralization may have been derived by lateral secretion from the andalusite schist. The average value of 50 ppm (Lindqvist, op. cit.) may come from samples within the depleted aureole. To obtain an accurate idea of whether this process has occurred one must sample outside the aureole.

The deposits at Wheal Ellen and South Hill are parallel to both So and S1. If the base metal content is anomalously high in the andalusite schist then it would suggest a stratiform origin for the deposits. However, if the base metal values are low adjacent to the deposit then lateral secretion from adjacent wall rocks may have occurred.

Two sections across the andalusite schist at South Hill were studied for the Cu-Pb-Zn content and compared to results from drill hole No. 7 at Wheal Ellen measured by Northern Mining.

A highway cutting, 100 m from the mineralization appeared suitable as it is a sufficient distance away to be outside of a lateral secretion aureole if one exists. Drill hole SH1, also studied, is close to the mineralization (less than 30 m away along strike). It is the longest hole and intersects all the major lithologies, and is below the weathering zone so that anomalous values derived by weathering of sulphides would be minimal.

Northern Mining drill hole 7 is a sufficient distance from the mineralization to be not affected by base metal depletion and is below the weathering zone so should not be affected by weathering as would the highway cutting at South Hill.

8.2 Investigation Procedure

For the highway cutting, 32 samples at 7.6 m (25') intervals were taken to include the 60 m wide andalusite schist. The andalusite schist horizon is not always massive, as 2 m interbeds of quartz-mica and biotite schists are included.

Twenty one samples from drill hole SH1 were taken, beginning at the approximate base of the weathering zone and including as many andalusite schist samples as possible.

The samples collected were crushed and ground using a jaw crusher and Sieb Technic Mill. The product was leached using perchloric acid and the measurements carried out using an atomic absorption spectrophotometer. For further details of the analytical procedure see Appendix 3.

Samples were selected from quartz-mica, biotite and andalusite schists at South Hill and Wheal Ellen as well as from pyritic schists from the latter. The lithological descriptions of the core from the Northern Mining drilling report doesnot allow the separate categorization of quartz-mica and biotite schists, therefore, they have been placed together under the one heading of quartz-mica schist.

8.3 Discussion of Results

Results of the rock sample survey are displayed in Figs. 11, 12 and 13. The average values and range, in brackets, are given for the lithologies at each locality and are as follows on the following page. Lindqvist (1969) suggested the quartz-mica schist to be originally a greywacke and the andalusite and biotite schists to be shales. The background values for shale, black shale and sandstone (Hawkes and Webb 1962) see Table 5 are compared to those obtained in this study.

It can be seen from Table 5 (on the following page) that the Cu-Pb-Zn values of the schists (except the pyritic schist) irrespective of its proximity to the mineralization is within the range of shales and sand-

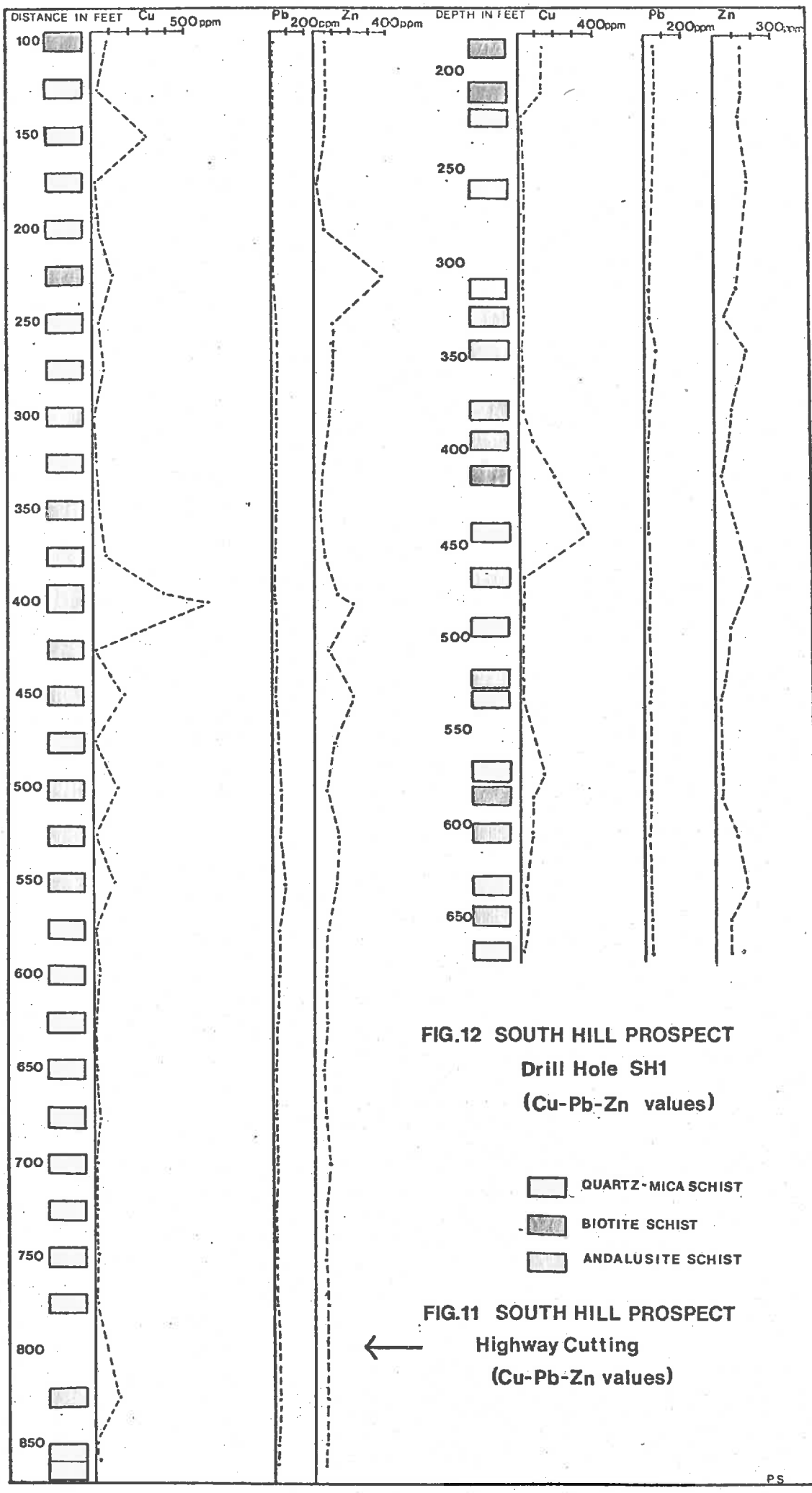

FIG.12 SOUTH HILL PROSPECT
Drill Hole SH1
(Cu-Pb-Zn values)

FIG.11 SOUTH HILL PROSPECT
Highway Cutting
(Cu-Pb-Zn values)

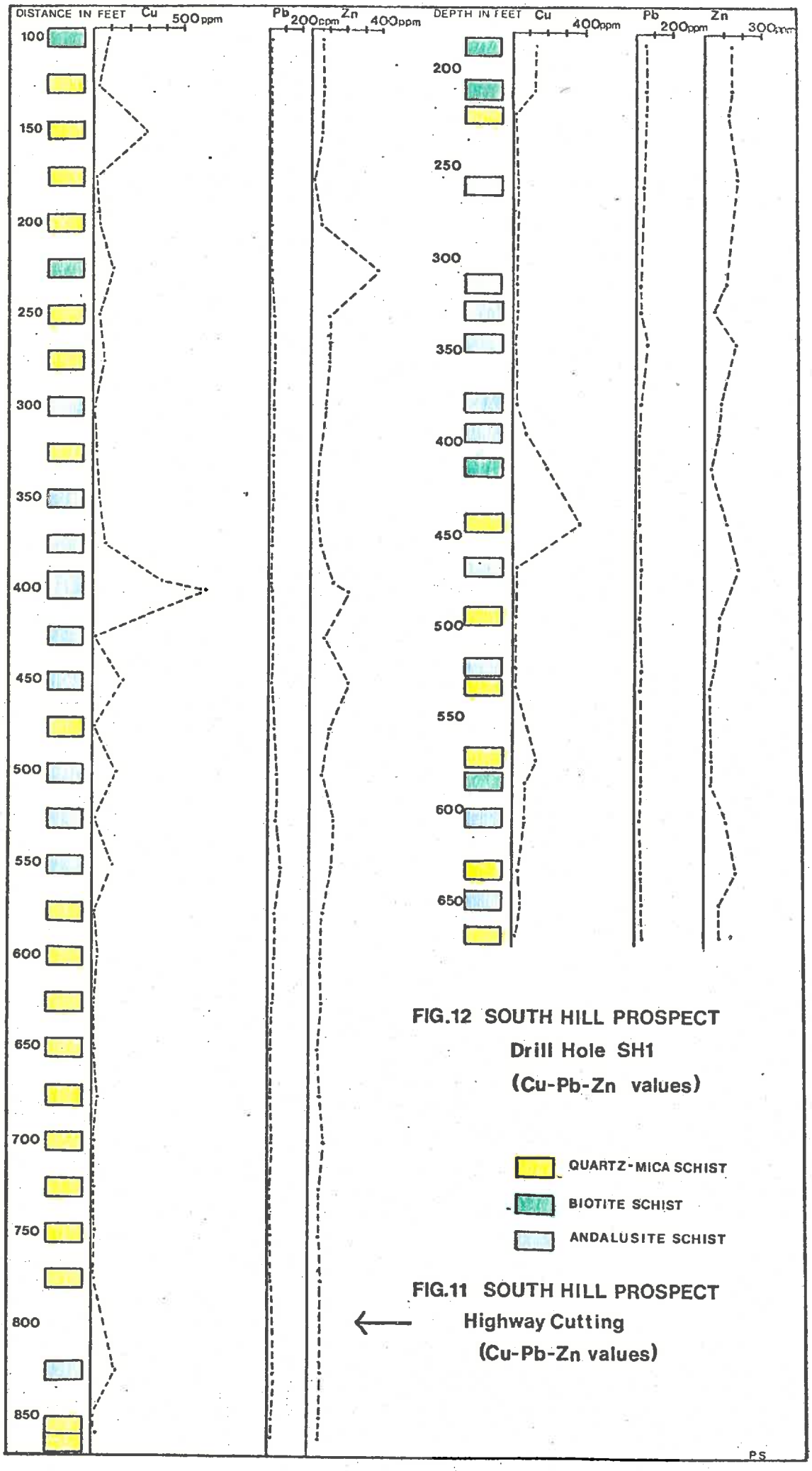

FIG.12 SOUTH HILL PROSPECT
Drill Hole SH1
(Cu-Pb-Zn values)

FIG.11 SOUTH HILL PROSPECT
Highway Cutting
(Cu-Pb-Zn values)

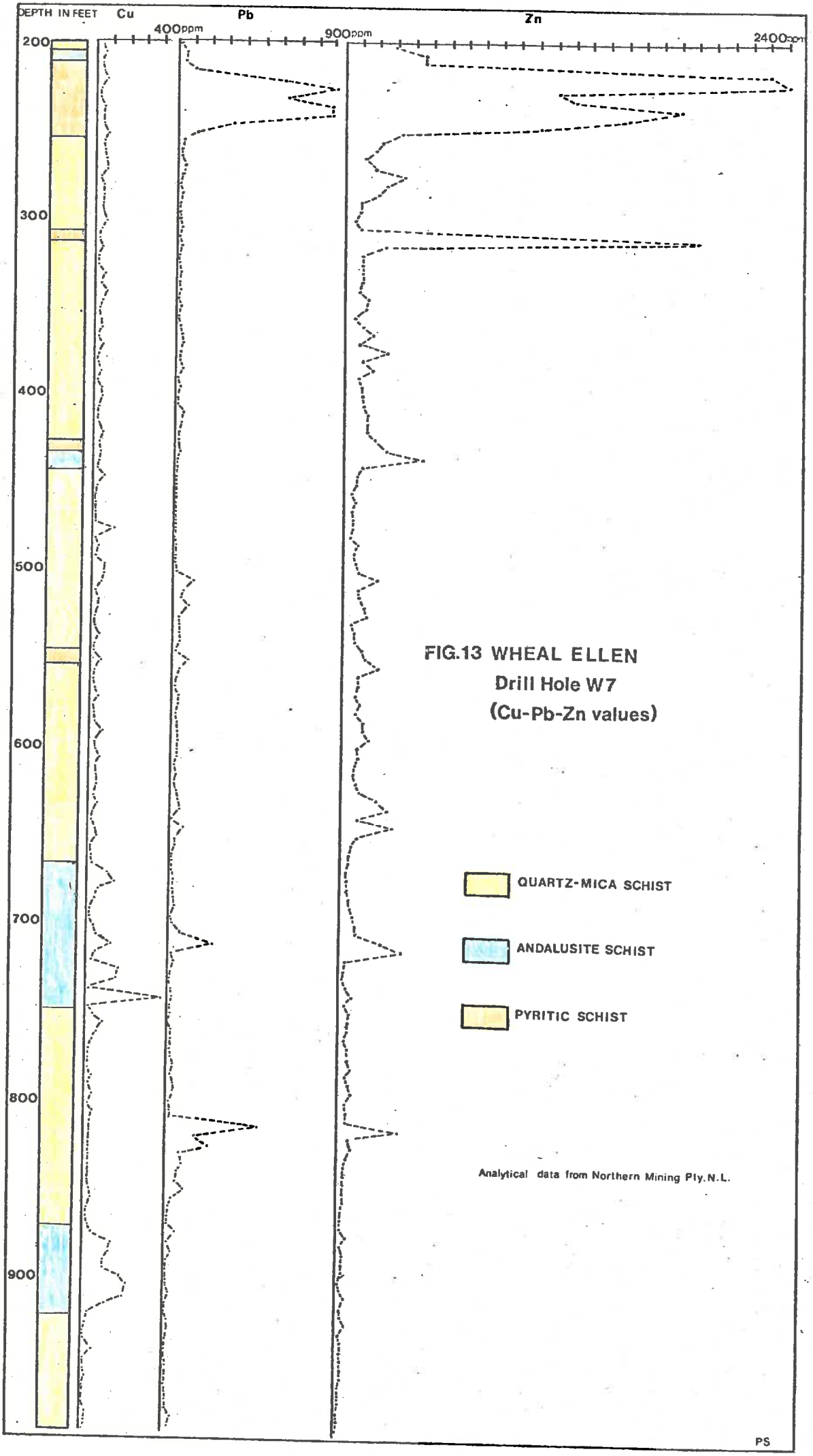

FIG.13 WHEAL ELLEN
Drill Hole W7
(Cu-Pb-Zn values)

Analytical data from Northern Mining Pty.N.L.

PS

stones (possibly greywackes also).

TABLE 4

Average values and range of lithologies (Cu-Pb-Zn)

	Cu ppm	Pb ppm	Zn ppm	no. of samples
South Hill : highway cutting				
Quartz-mica schist	33 (2-200)	15 (2-50)	68 (28-115)	19
Biotite schist	71 (17-110)	13 (8-24)	175 (65-370)	3
Andalusite schist	165 (4-610)	32 (5-67)	106 (59-220)	10
South Hill : drill hole SH1				
Quartz-mica schist	67 (6-259)+	26 (18-48)	83 (23-131)	7
Biotite schist	125 (68-190)	22 (12-28)	91 (35-147)	4
Andalusite schist	28 (12- 39)	38 (22-64)	113 (49-173)	10
Wheal Ellen : drill hole W7x				
Quartz-mica schist	30	25	98	120
Pyritic schist	36	501	1582	12
Andalusite schist	83	34	71	25

\+ 1 high value due to Fe stained quartz vein in sample

x bulked samples averaged over 1.52 m (5') intervals

TABLE 5

Average values for some sedimentary rocks (Cu-Pb-Zn)

	Cu ppm	Pb ppm	Zn ppm
Sandstone	10- 40	10- 40	5- 20
Shale	30-150	20	50- 300
Black Shale	20-300	20-400	100-1000

(Hawkes and Webb, 1962)

8.4 Conclusions

1. The Cu content of the andalusite schist is too low for the Wheal Ellen and South Hill deposits too have been soley derived from it. This tends to not favour syngenetic origins for the mineralization in view of the anomalously high Cu values observed for the Ukaparinga schist when compared to the andalusite schist.
2. The base metal content for all lithologies is close to averages expected if they were originally shales, sandstones and greywackes, except for the pyritic schist which is anomalously high. The pyritic schist may have been a black shale in which case the Cu-Pb-Zn

values are only at most double that expected for this lithology.

3. The process of lateral secretion of base metals from andalusite schist does not appear to have taken place since within the possible diffusion aureole (drill hole SH1) and outside of the aureole (South Hill highway cutting and drill hole W7) the Cu-Pb-Zn values are within the range of values for a shale (Hawkes and Webb, op. cit.).
4. The volume of sulphide at South Hill, Kanmantoo and Wheal Ellen is not too great to overrule the possibility of having been derived from all lithologies and not just the andalusite schist.

CONCLUSIONS

The schists enclosing the mineralized areas in the Kanmantoo Group were originally a greywacke-shale sequence with flysch-like characteristics.

Three deformations, and possibly a fourth, appear to be related to the metamorphic history in the following way. Sediments reached mid-amphibolite grade during the early stages of the Delamerian orogeny as shown by the presence of pre S1 andalusites. The presence of Si in pre S1 andalusites discordant to Se (S1) and of mullion like structures (Poole, 1969) may be evidence of a deformation prior to that producing the dominant S1 schistosity.

Peak metamorphic conditions were reached during and just after the production of S1 as shown by the presence of syntectonic andalusites and fibrolite and post-S1 andalusite, staurolite, garnet, biotite and muscovite. The metamorphic assemblages suggest temperatures of between 500 and 640°C and pressures between 1.8 and 3.8 kb depending on the alumino-silicate curve chosen (Newton, 1966 a and b; Holdaway, 1971). Short relaxations of compressive forces during F1 resulted in the formation of quartz veins parallel to S1. Two deformations at quartz-muscovite-biotite grade followed each producing non penetrative crenulation cleavages. Kinking, faulting and minor shearing were produced late in the history.

The presence of flattened sulphides disseminated in all metamorphic assemblages, mesoscopic folded layers parallel to bedding (Askins, 1968) and flattened recrystallized sulphides within metamorphic layers that probably represented bedding suggest that sulphides were either present as sedimentary components or were formed in the earliest stages of metamorphism.

Mineralization appears to have taken place during the first deformation in all areas as suggested by the relationship of mineralized quartz veins parallel to S1 or in possible conjugate shears produced during F1 at Bremer.

Sulphur isotope studies suggest a hydrothermal origin for Wheal Ellen, Strathalbyn, South Hill Prospect, Bremer, Kanmantoo deposits and adjacent areas. The metamorphically derived fluids in each area having different proportions of meteoric and sea water as shown by the consistency of range between +0 and +20. The contribution of hydrothermal fluids is unknown due to the absence of any magmatic body in the vicinity of the mineralized areas. Negative values of the Nairne Pyrite Formation and thin pyritic schists throughout the Kanmantoo Group

suggest the sulphides contained are syngenetic and have sulphur of biological origin.

A few sulphides from the deposits have negative sulphur isotope values probably due to local variation in Eh, pH or T conditions. The sulphur isotope values suggest an abiological origin unrelated to the pyrite horizons.

P-T conditions as deduced from sphalerite geobarometry and sulphur isotopes indicate that sulphides have reequilibrated below the temperature peak near a temperature of 420°C. A pressure of 4.4 (±0.5) kb is slightly above that deduced by silicate stabilities and probably represents the pressure of regional metamorphism. If considered too high then it may be due to submicroscopic Cu in the sphalerite lattice.

The andalusite schist does not appear to be the sole source for the sulphides therefore an alternative explanation must be given for its significance.

Andalusites had crystallized before S1, therefore the presence of the prophyroblasts within selected units could mean that for a given shear stress the resulting strain is different in adjacent lithologies. The differential movement during the formation of S1 in reaching the metamorphic peak may have produced shears, in, or adjacent to, the andalusite schist due to inhomogeneities. These minor shears may be the loci for the mineralizing solutions.

The relationships of mineralization to a metamorphic horizon is not unique. Magee (1970) noted the relationships of the staurolite schist to the ore horizons in the Ducktown District, Tennessee. This district has such a large number of features in common with the Kanmantoo District that they are worth listing here:

(1) Rocks belong to the amphibolite facies, the key minerals are kyanite, staurolite and andalusite.
(2) No association of mineralization with an igneous body.
(3) Sulphide assemblage is pyrite, pyrrhotite, chalcopyrite, sphalerite and magnetite.
(4) Lithologies are similar: mica schists, greywackes, sericite schists that contain up to 20% pyrite and pyrrhotite.
(5) The Boyd ore body has an envelope of chlorite-garnet schist below the 10 level.
(6) Mineralization is associated with shears and "replacement" of favourable zones in large fold structures according to Magee (op. cit).
(7) Conflicting origins - (i) hydrothermal replacement of particular

horizons (Emmons and Laney, 1926; Ross, 1935), (ii) syngenetic, (iii) hydrothermal solutions concentrating in shears, Magee (op. cit.)

(8) Metamorphism before localization of mineralization (Magee, op. cit.)

(9) Sulphur isotope values 0 to +10 per mil (Mauger, 1972).

Carpenter (1970) showed that the massive sulphide lenses and kyanite zones are roughly coincident with an area of tight folding. As a result the staurolite and kyanite may create zones of weakness into which mineralization is concentrated.

The sulphide deposits are probably epigenetic resulting from mobilization of disseminated sulphides in the country rock by siliceous fluids. These metamorphically derived fluids were then localized into shear zones and tightly folded areas such as is the case at Kanmantoo and Aclare. Mobilization took place early in F1 as shown by the mineralized quartz veins parallel to S1. This was followed later in F1 by solid state movement of the sulphides as indicated by the flattened sulphides parallel to S1 and concentration of sulphides in hinge zones of minor folds.

ACKNOWLEDGEMENTS

The project was suggested and supervised by Dr. R. Both and I express my thanks to him for his invaluable discussion and assistance throughout the year.

Financial assistance from Western Mining Corporation Ltd., Utah Development Company and the South Australian Mines Department was greatly appreciated.

Special thanks are extended to Dr. A. Spry, my father, for his comments and criticisms throughout the year and his aid in compilation.

I am indebted to Northern Mining Pty. Ltd., in particular B. Morgan and to D.O'Connor from Mines Exploration Pty. Ltd. for the use of drill core and access to unpublished material.

Thanks also go to staff and fellow students for their useful discussion but particularly Professor P. Ypma, Dr. S. Scott, G. Teale, M. Jones, N. Mancktelow and R. Roberts.

Finally, I would like to express my gratitude to J. Drexal from the South Australian Mines Department for his close interest in the project and his useful comments.

REFERENCES

ALTHAUS, E. 1969. Das system Al_2O_3-SiO_2-H_2O. Experimentelle untersuchungen and folkerungen fur die petrogenese der metamorphen. Gestein. Neus Jb. Miner. Abh., 111, p. 74-110.

ANGER, G., NIELSEN, H., PUCHELT, H. and RICKE, W. 1966. Sulfur isotopes in the Rammelsberg ore deposit (Germany). Econ. Geol., 61, p. 511-536.

ASKINS, P.W. 1968. Geochemical exploration around the Aclare Mine and mineral deposits of the surrounding region. Unpub. B.Sc. Hons. thesis, University of Adelaide.

AUSTIN, J.B. 1863. The mines of South Australia. Pub. in Adelaide, p. 80-81.

CARMICHAEL, D.M. 1969. On the mechanism of prograde metamorphic reactions in quartz-bearing silicates. Contr. Miner. Petrology, 20, p. 244-267.

CARPENTER, R.H. 1967. Regional metamorphism in the Western Blue Ridge of Tennessee and North Carolina. Tenn. Val. Auth., Knoxville.

COCHRANE, G.W. 1954. Strathalbyn Mine. Dept. Mines S.Aust. Mining Review, 97, p. 95-98.

COCHRANE, G.W. 1956. Diamond drilling, Wheal Ellen silver-lead mine. Dept. Mines S.Aust. Mining Review, 99, p. 29-32.

DAILEY, B. and MILNES, A.R. 1972A. Revision of the stratigraphic nomenclature of the Cambrian Kanmantoo Group, South Australia. J. Geol. Soc. Aust., 19(2), p. 197-202.

DAILEY, B. and MILNES, A.R. 1973. Stratigraphic, structure and metamorphism of the Kanmantoo Group (Cambrian) in its type section east of Tunkalilla Beach, South Australia. Trans. Roy. Soc. S.Aust., 97, p. 213-242.

DICKINSON, S.B. 1942. The structural control of ore deposition in some South Australian copper deposits. Geol. surv. S.Aust. Bull. 20.

DUNCAN, N. 1973. Exploration at the Bremer Mine, Callington, South Australia. Unpub. report to Northern Mining Pty. N.L.

EMMONS, W.H. and LANEY, F.B. 1926. Geology and ore deposits of the Ducktown mining district, Tennessee. U.S. Geol. Surv. Prof. Paper, 139, p. 114.

FLEMING, P.D. 1971. Metamorphism and folding in the Mt. Lofty Ranges, South Australia, with particular reference to the Dawesley-Kanmantoo area. Unpub. Ph.D. thesis, University of Adelaide.

GEORGE, R.J. 1967. Metamorphism of the Nairne Pyrite Deposit. Unpub. Ph.D. thesis, University of Adelaide.

GRASSO, R. and McMANUS, J.B. 1954. The geology of the Callington Area. Unpub. B.Sc. Hons. thesis, University of Adelaide.

GROOTENBOER, J. and SCHWARCZ, H.P. 1969. Temperature dependent sulfur-isotope fractionation between sulfide minerals. Earth Planet. Sci. Lett., 7, p. 162-166.

GROVES, D.I., BINNS, R.A., BARRETT, F.M. and McQUEEN, K.G. 1975. Sphalerite compositions from Western Australian nickel deposits, a guide to equilibria below 300°C. Econ. Geol., 70, p. 391-396.

GROVES, D.I., BINNS, R.A., BARRETT, F.M. and McQUEEN, K.G. 1976. Application of sphalerite geobarometry and sulfur isotope geothermometry to ores of the Quemont Mine, Noranda, Quebec. Discussions. Econ. Geol., 71, p. 949-950.

HAWKES, H.E. and WEBB, J.S. 1962. Geochemistry in mineral exploration. New York, Harper and Row.

HENLEY, K.J. and BROWN, R.N. 1974. Cupriferous hydrobiotite from Ukaparinga, South Australia. Econ. Geol., 69, p. 688-692.

HOBBS, B.E. 1975. The Broken Hill lode horizon project. Unpub. report by Monash University ore deposits study group to Broken Hill Mining Managers' Association.

HOLDAWAY, M.J. 1971. Stability of andalusite and the aluminium silicate phase diagram. Am. J. Sci., 271, p. 97-131.

HOSCHEK, G. 1967. Zur unteren stabilitätsgrenze von staurolith. Naturwissenschaften, 54, p. 200.

HOSCHEK, G. 1968. Zur oberen stabilitätsgrenze von staurolith. Naturwissenschaften, 55, p. 226-227.

HOSCHEK, G. 1969. The stability of staurolite and chloritoid and their significance in metamorphism of pelitic rocks. Contr. Miner. Petrology, 22, p. 208-233.

HSU, L.C. 1968. Selected phase relationships in the system Al-Mn-Fe-Si-O-H: A model for garnet equilibria. J. Petrology, 9, p. 40-83.

JENSEN, M.L. and WHITTLE, A.W.G. 1969. Sulfur isotopes of the Nairne Pyrite Deposit, South Australia. Mineral. Deposita, 4, p. 241-247.

JONES, D.G. 1975. The Ukaparinga Schist: A copper-bearing biotite schist near Williamstown, South Australia. Unpub. M.Sc. thesis, University of Adelaide.

JONES, H. 1913. Strathalbyn copper and silver-lead Mine. Dept. Mines S.Aust. Mining Review, 18, p. 33-35.

KAJIWARA, Y. and KROUSE, H.R. 1971. Sulfur isotope partitioning in metallic sulfide systems. Canad. Jour. Earth Sci., 8, p. 1397-1408.

KAJIWARA, Y., KROUSE, H.R. and SASAKI, A. 1969. Experimental study of sulfur isotope fractionation between coexisting sulfide minerals. Earth. Planet. Sci. Lett., 7, p. 271-277.

KLEEMAN, A.W. and SKINNER, B.J. 1958. The Kanmantoo Group in the Strathalbyn-Harrogate Region, South Australia. Trans. Roy. Soc. S.Aust., 82, p. 61-71.

LA GANZA, R.F. 1959. The Nairne sulphide deposit. Unpub. M.Sc. thesis, University of Adelaide.

LINDQVIST, W.F. 1969. Geology and metamorphic history of the Kanmantoo Copper Deposit, South Australia. Unpub. Ph.D. thesis, University of London.

LUSK, J. 1972. Examination of volcanic-exhalative and biogenic origins for sulfur in the stratiform massive sulfide deposit of New Brunswick. Econ. Geol., 67, p. 169-183.

LUSK, J. 1976. Application of sphalerite geobarometry and sulfur isotope geothermometry to ones of the Quemont Mine, Noranda, Quebec - A reply. Econ. Geol., 71, p. 949-950.

LUSK, J., CAMPBELL, F.A. and KROUSE, H.R. 1975. Application of sphalerite geobarometry and sulfur isotope geothermometry to ores of the Quemont Mine, Noranda, Quebec. Econ. Geol., 70, p. 1070-1083.

LUTH, W.C., JAHNS, R.H. and TUTTLE, O.F. 1964. The granite system at pressures of 4 to 10 kilobars. J. Geophys. Res., 69, p. 759-777.

MAGEE, M. 1970. Geology and ore deposits of the Ducktown District, Tennessee. In Ore deposits of the United States, 1933-1967 (ed. J.D. RIDGE), New York, Amer. Instit. Min. Metall. Petroleum Engineers, Inc.

MARLOW, P.C. 1975. Structural investigations of the Kanmantoo Group metasediments near Macclesfield, South Australia. Unpub. M.Sc. thesis, University of Adelaide.

MAUGER, R.L. 1972. A sulfur isotope study of the Ducktown Tennessee District. U.S.A. Econ. Geol., 67, p. 497-510.

McDONALD, J.A. 1967. Metamorphism and its effects on sulfide assemblages. Mineral. Deposita., 2, p. 200-220.

McDONALD, J.A. 1970. Some effects of deformation on sulfide-rich layers in lead-zinc ore bodies, Mount Isa, Queensland. Econ. Geol., 65, p. 273-298.

MIRAMS, R.C. 1962. The geology of the Mount Barker - Callington area. Dept. of Mines S.Aust. Mining Review, 117, p. 9-16.

MIRAMS, R.C. 1965. Pyrite-pyrrhotite deposit at Nairne. In Geology of Australian ore deposits (ed. McANDREW). 8th Comm. Min. Metall. Congr., Aust. and N.Z., p. 316-318.

MISCH, P. 1971. Porphyroblasts and crystallization: Some textural criteria. Geol. Soc. Amer. Bull., 82, p. 245-251.

NEWTON, R.C. 1966A. Kyanite-sillimanite equilibrium at 750°C. Science, 151, p. 1222-1225.

NEWTON, R.C. 1966B. Kyanite-andalusite equilibrium from 700° to 800°C. Science, 153, p. 170-172.

OFFLER, R. 1960. The structure, petrology and stratigraphy of the Strathalbyn Anticline, South Australia. Unpub. B.Sc. Hons. thesis, University of Adelaide.

OFFLER, R. 1963. Structural geology of the Strathalbyn Anticline, South Australia. Trans. Roy. Soc. S.Aust., 87, p. 199-208.

OFFLER, R. and FLEMING, P.D. 1968. A synthesis of folding and metamorphism in the Mt. Lofty Ranges, South Australia. J. Geol. Soc. Aust., 15, p. 245-266.

OHMOTO, H. 1972. Systematics of sulfur and carbon isotopes in hydrothermal ore deposits. Econ. Geol., 67, p. 551-578.

PETTIJOHN, F.J. 1957. Sedimentary Rocks. New York, Harper and Bros.

POOLE, L.E. 1969. The structural geology of an area south of Kanmantoo, South Australia. Unpub. B.Sc. Hons. thesis, University of Adelaide.

RAMDOHR, P. 1969. The ore minerals and their intergrowths. Oxford, Pergamanon Press.

RAMSAY, J.G. 1967. Folding and fracturing of rocks. New York, McGraw-Hill.

RICHARDSON, S.W. 1968. Staurolite stability in a part of the system Fe-Al-Si-O-H. J. Petrol., 9, p. 467-488.

RICHARDSON, S.W., GILBERT, M.C. and BELL, P.M. 1969. Experimental determination of kyanite-andalusite and andalusite-sillimanite equilibria; the aluminium silicate triple point. Am. J. Sci., 267, p. 259-272.

ROBINSON, B.W. and OHMOTO, H. 1973. Mineralogy, fluid inclusions and stable isotopes of the Echo Bay U-Ni-Ag-Cu deposits, Northwest Territories, Canada. Econ. Geol., 68, p. 635-656.

ROSS, C.S. 1935. Origin of the copper deposit of the Ducktown type in the Southern Appalachian region. U.S. Geol. Surv. Prof. Paper, 179, p. 165.

RYE, R.O. and OHMOTO, H. 1974. Sulfur and carbon isotopes and ore genesis. Econ. Geol., 69, p. 826-842.

SCOTT, S.D. 1973. Experimental calibration of the sphalerite geobarometer. Econ. Geol., 68, p. 466-474.

SCOTT, S.D. and BARNES, H.L. 1967. Sphalerite geothermometry at 330° to 580°. Econ. Geol., 62, p. 874-875.

SCOTT, S.D. and BARNES, H.L. 1969. Sphalerite geobarometer. Geol. Soc. Amer., Abstracts, 7, p. 202.

SCOTT, S.D. and BARNES, H.L. 1971. Sphalerite geothermometry and geobarometry. Econ. Geol., 66, p. 653-669.

SKINNER, B.J. 1958. The geology and metamorphism of the Nairne Pyrite Formation, a sedimentary sulfide deposit in South Australia. Econ. Geol., 53, p. 546-562.

SPRIGG, R.C. and CAMPANA, B. 1953. The age and facies of the Kanmantoo Group. Aust. J. Sci., 16(1), p. 12-14.

SPRY, A. 1969. Metamorphic textures. Oxford, Pergamanon Press.

SPRY, A. 1972. Porphyroblasts and 'crystallization force': Some textural criteria: Discussion. Geol. Soc. Amer. Bull., 83, p. 1201-1202.

STANTON, R.L. 1964. Mineral interfaces in stratiform ores. Trans. Inst. Min. Metall., 74, p. 45-79.

STANTON, R.L. 1972. Ore petrology. New York, McGraw-Hill.

STANTON, R.L. and RAFTER, T.A. 1966. The isotopic constitution of sulfur in some stratiform lead-zinc sulphide ores. Mineral. Deposita., 1, p. 16-29.

VERWOERD, P.J. and CLEGHORN, J.H. 1975. Kanmantoo copper ore body. Aust. Inst. Min. Metall. Monograph, 5, p. 560-565.

VOKES, F.M. 1968. Regional metamorphism of the Palaeozoic geosynclinal sulphide ore deposits of Norway. Trans. Inst. Min. Metall., 77, p. 53-59.

VOKES, F.M. 1971. Some aspects of the regional metamorphic mobilization of pre-existing sulfide deposits. Mineral. Deposita., 6, p. 122-129.

WADE, M.L. and COCHRANE, G.W. 1952. Wheal Ellen Mine. Dept. Mines S.Aust. Mining Review, 97, p. 68-81.

WINKLER, H.G.F. 1974. Petrogenesis of metamorphic rocks. Springer-Verlag, New York Inc.

ZWART, H.J. 1960. Relations between folding and metamorphism in the Central Pyrenees, and their chronological succession. Geologie Mijnb., 39e, p. 163-180.

APPENDIX I

SPHALERITE GEOBAROMETRY

1. Introduction

Sphalerite samples were obtained from drill holes and dump materials.

Sample No.	Exact Locations
501/062	Wheal Ellen DDH4 375'
501/035	Wheal Ellen surface dump
501/036	Wheal Ellen surface dump
501/037	Wheal Ellen surface dump
501/061	Wheal Ellen DDH4 361'5"
501/064	Wheal Ellen DDH4 359'8"
501/110	Wheal Ellen surface dump
501/047	South Hill Prospect SH7 290'
501/041	South Hill Propsect SH7 291'
501/044	Bremer surface dump
501/042	Bremer surface dump
501/054	500 m north of Kanmantoo Mine: KS 40 2167'
501/055	3200 m north of Kanmantoo Mine: KS 123 137'
KS40 2135′	500 m north of Kanmantoo Mine: KS 40 2135'
ST 1 207′	Strathalbyn ST1 207′

More than 30 polished sections were initially examined for the presence of sphalerite but only 20 of these were found to contain the mineral; the sphalerite grains were usually circled to make their location with the electronprobe easier. Aid in sample selection was carried out by F. Radke while the microprobe analyses were carried out by P.K. Schultz, both of Amdel. Of these 20 polished sections 15 were analysed.

The dominance of hexagonal pyrrhotite at Kanmantoo (Lindqvist (1969)), which was analysed by x-ray diffraction, and Nairne (Skinner, 1958) in addition to testing with magnetic colloid suggests that nearly all the pyrrhotite is hexagonal and not monoclinic.

2. Experimental Procedure

All polished sections were carbon coated prior to analysis and then analysed using an electron beam of 2-3 microns diameter, generated by an accelarating voltage of 20 kv and giving a specimen current of about .07 micro amps.

At least three point analyses were carried out in all samples using pure metal standards for all elements except Zn and S, for which a pure

sphalerite sample was used. All the results obtained were corrected by computer for atomic number, mass absorption and secondary fluorescent effects.

3. Results.

Lead was not detected in any of the sphalerites analysed, but the detection limit for lead in sphalerite was only about 0.5% due to the interference of the SKα line with the Pb Mα line.

Copper was also not detected (at the detection limit of 0.2%) in all samples except for small grains (<50 microns) present in a sphalerite matrix which showed detectable Cu. This most probably came from the adjacent chalcopyrite.

Cd and Mn were detected in some sphalerites at detection levels of 0.1% and .02% respectively.

No definite compositional variations were detected within any given samples, therefore the individual point analyses of each sample were averaged and only one final analysis is given for each sample.

ELECTRON MICROPROBE ANALYSES OF FIFTEEN SPHALERITES

Sample No.	Mol Wt% Fe S	Cd Wt.%	Zn Wt.%	Fe Wt.%	Mn Wt.%	S Wt.%	Total Wt.%
501/036	15.36	0.17	57.6	9.0	0.28	32.7	99.75
501/035	15.41	0	57.1	9.0	0.62	33.0	99.72
501/036	15.08	0	57.7	8.8	0.27	32.8	99.37
501/037	15.24	0	57.6	8.9	0.30	32.9	99.70
501/061	15.22	0.17	57.6	8.9	0.30	32.9	99.87
501/064	15.06	0	57.7	8.8	0.29	33.0	99.79
501/110	15.12	0	57.5	8.8	0.20	32.8	99.30
501/047	10.87	0.27	60.2	5.9	0.02	33.2	99.59
501/046	9.91	0.24	60.5	5.7	0.02	33.0	99.46
501/044	13.79	0.88	57.3	7.9	0.03	32.7	98.81
501/042	14.14	2.4	55.9	8.1	0.02	32.7	99.12
501/054	10.41	0	60.4	6.0	0	33.1	99.5
501/055	10.60	0	60.0	6.2	0	33.2	99.4
ST1 207	-	0	64.3	1.1	0	33.1	98.5
KS40 2135	-	0	65.0	2.1	0	33.0	100.1

Chemical composition of sphalerites in equilibrium with pyrite and pyrrhotite at Shephards Hill Quarry. (Skinner, 1958)

No	Zn%	Fe%	Mn%	Cd%	Cu	Mol% FeS
S1 1	55.1	9.0	2.3	0.19	<0.03	15.3
S1 2	55.0	8.8	2.5	0.18	<0.03	15.1

APPENDIX 2

SULPHUR-ISOTOPE STUDY : Experimental Procedure

Sulphides were collected from dump material at Wheal Ellen whereas outcrop samples were obtained from the Nairne Pyrite Formation. Kanmantoo Mines supplied drill core for South Hill and the Kanmantoo area while Northern Mining Limited and the South Australian Mines Department made drill core available for Wheal Ellen work.

As the sulphides were fine grained or disseminated, the samples were crushed and ground using a jaw crusher and disc grinder. The material was sieved and the -60 to +170 content was kept. Sulphides were then separated by a superpanner and Franz Isodynamic Magnetic Separator. One problem encountered using the latter was due to the presence of fine disseminated magnetite in the pyrite fraction which resulted in pyrite showing similar magnetic response to pyrrhotite.

Final purities were greater than 90% with silicate being the major component. In all cases greater than 97% purity with respect to sulphides were obtained.

The weighed samples were burnt in excess cupric oxide for greater than ten minutes to produce sulphur dioxide. Non condensables were removed by freezing and over a liquid nitrogen trap. Water and then CO_2 were removed by passing the gas over a dry ice-acetone mixture and n-pentane slurry respectively.

The sulphur isotope ratios were measured using a Micromass 602C gas source mass spectrometer in the Antarctic Research Division at the University of Melbourne. The results are given in per mil

$$\delta^{34}\text{S(per mil)} = \left(\frac{^{34}S/^{32}S \text{ sample}}{^{34}S/^{32}S \text{ standard}} - 1\right).1000$$

The standard is the troilite from the Cañon Diable meteorite whose accepted ratio is 0.0450045. The precision for the $\delta^{34}S$ results is ±0.2 per mil hence for $\Delta\delta^{34}S$ is ±0.4 per mil. Periodic checks with sulphides of known $\delta^{34}S$ were carried out. The sulphides were Broken Hill galena ($\delta^{34}S$ = + 2.8 per mil), Fisher Reagent zinc sulphide (δ^{34} = + 22.0 per mil) and a Mississippi Valley sphalerite ($\delta^{34}S$ = - 6.7 per mil).

RESULTS OF SULPHUR-ISOTOPE STUDY

WHEAL ELLEN MINE

			$\delta^{34}S$ (per mil)
No. 11	gn	036	+2.72
No. 12	gn	036	+1.96
No. 63	sp	036	+3.70
No. 4	sp	036	+4.34
No. 64	gn	035	+1.92
No. 28	gn	035	+2.46
No. 58	sp	035	+3.85
No. 23	gn	038	+2.63
No. 27	py	060	+6.51
No. 8	py	039	+2.40
No. 1	po	039	+2.31
No. 19	po	060	+4.52
No. 21	sp	061	+4.55
No. 9	py	039	+2.41
No. 32	py	110	+4.48
No. 36	py	110	+3.87
No. 33	sp	110	+3.84

WHEAL ELLEN PYRITIC SCHIST

No. 57	py	W3A	204'2"	-15.14
No. 56	py	W3	310'4"	-18.67
No. 42	py	W3	305	-20.09
No. 47	py	W3	310'10"	-15.06
No. 61	py	W3	305	-19.67
No. 44	py	W3	297	-16.30
No. 49	py	W3	310'4"	-18.34

NAIRNE PYRITE FORMATION

No. 46	py		-15.40
No. 62	py		-16.30

KANMANTOO MINE

			$\delta^{34}S$ (per mil)
No. 55	cpy	050	+9.56
No. 34	cpy	051	+9.87
No. 37	po	051	+9.74
No. 24	cpy	052	+15.53
No. 41	cpy	052	+16.12
No. 65	py	052	+16.15

STRATHALBYN MINE

No. 31	py	059	-4.72
No. 2	py	057	+2.83
No. 38	py	058	-0.03
No. 13	py	056	-3.32

BREMER MINE

No. 51	cpy	123	+1.55
No. 3	cpy	042	+0.89
No. 5	py	042	+1.29
No. 54	cpy	124	-3.14

SOUTH HILL PROSPECT

No. 10	py	046	-3.06
No. 18	po	046	+2.53
No. 6	py	047	-0.47
No. 25	py	045	+3.89
No. 7	cpy	049	+3.14

NOMENCLATURE

po - pyrrhotite; cpy - chalcopyrite; py - pyrite

Sp - sphalerite; gn - galena

Temperatures.

Five different sulphide pairs were used to calculate temperatures from the deposits. Three sulphide pairs were analysed at Wheal Ellen and each from South Hill Prospect, Bremer and the Kanmantoo Area.

The $\Delta\ \delta^{34}S$ for each mine is given below.

					$\Delta\ \delta^{34}S$	$T^{o}C$
WHEAL ELLEN						
No. 11	gn	036	+2.72	} 2.34		
No. 12	gn	036	+1.96		1.68	417
No. 63	sp	036	+3.70	} 4.02		
No. 4	sp	036	+4.34			
No. 64	gn	035	+1.90	} 2.19		
No. 28	gn	035	+2.46		1.66	421
No. 58	sp	035	+3.85			
No. 27	py	060	+6.51			
No. 19	po	060	+4.52		1.99	115
No. 8	py	039	+2.40			
No. 1	po	039	+2.31		0.09	1553
No. 32	py	110	+4.48	} 4.17		
No. 36	py	110	+3.87		0.33	680
No. 33	sp	110	+3.84	3.84		
SOUTH HILL PROSPECT						
No. 10	py	046	-3.06			
No. 18	po	046	+2.53		5.59	-
BREMER						
No. 13	cpy	042	+0.89			
No. 5	py	042	+1.29		0.40	788
KANMANTOO AREA						
No. 34	cpy	051	+9.87			
No. 37	po	051	+9.74		0.13	1588

The temperatures have been derived using equations from Kajiwara and Krouse (1971).

They are

1. $\Delta\ \delta^{34}S$ po - cp = $1.5 \times 10^{5}/T(^{o}K)^{2}$ ± 25% uncertainty

2. $\Delta\ \delta^{34}S$ py - cp = $4.5 \times 10^5/T(^oK)^2$ ± 10% uncertainty

3. $\Delta\ \delta^{34}S$ py - po = $3.0 \times 10^5/T(^oK)^2$ ± 15% uncertainty

4. $\Delta\ \delta^{34}S$ py - sp = $3.0 \times 10^5/T(^oK)^2$ ± 20% uncertainty

5. $\Delta\ \delta^{34}S$ sp - gn = $8.0 \times 10^5/T(^oK)^2$ ± 10% uncertainty

APPENDIX 3

Cu-Pb-Zn Atomic Absorption Analyses

Samples collected from the South Hill highway cutting were taken adjacent 25' pegs which were part of a Highways Department survey grid. Initially six quartz-mica schist samples and ten andalusite schist samples were analysed. These values did not give a suitable average for quartz-mica schist and did not include any biotite schist samples. A further sixteen samples were collected, one was taken adjacent the very high Cu sample (610 ppm) to check whether it was in error. The 310 ppm value of the "check" sample suggests the original sample to be correct.

Samples from South Hill drill hole 1 were taken from core material housed at Kanmantoo mines. Wheal Ellen drill hole 7 Cu-Pb-Zn data was obtained from Northern Mining. The values are from bulked samples over 1.52 m (5') intervals.

Experimental Procedure

The fresh rock samples were initially crushed by a disc grinder and Sieb Technic Mill for two minutes. 0.5 gm of sample was dissolved in 5 mls of perchloric acid (70%) and was then heated to at least 200°C for two days until 1 ml of solution remained. The perchloric acid leached all metallic ions from the silicate lattice. The resultant solution was made up to 20 ml by addition of distilled water.

Cu-Pb-Zn values were measured on a Techtron AA-3 atomic absorption spectrophotometer and the following performance data was used:

	Zn	Pb	Cu
Lamp Current	6.0 m A	8.0 m A	6.0 m A
Slit width	300 microns	300 microns	50 microns

Cu-Pb-Zn Values from South Hill Highway Cutting

Peg No. in feet	Cu	Pb	Zn	Sample Description
22,100	85	8	65	Biotite Schist
22,125	32	8	75	Quartz Mica Schist
22,150	300	5	65	Q Mi Sc i crosscutting Fe Q Veil
22,175	20	2	28	Quartz Mica Schist
22,200	45	2	55	Quartz Mica Schist
22,225	110	8	370	Biotite Schist
22,250	47	40	102	Quartz Mica Schist
22,275	71	46	115	Quartz Mica Schist
22,300	2	30	91	Andalusite Schist
22,325	24	30	55	Quartz Mica Schist
22,350	47	20	45	Andalusite Schist
22,375	63	24	59	Andalusite Schist
22,390	370	5	140	Andalusite Schist
22,400	610	30	220	Andalusite Schist
22,425	17	24	89	Biotite Schist i Ret An
22,450	155	34	219	Andalusite Schist
22,475	6	50	104	Quartz Mica Schist
22,500	144	46	79	Andalusite Schist
22,525	12	67	147	Andalusite Schist
22,550	104	38	136	Andalusite Schist
22,575	5	20	79	Quartz Mica Schist
22,600	32	16	61	Quartz Mica Schist
22,625	5	3	38	Quartz Mica Schist
22,650	8	12	50	Quartz Mica Schist
22,675	5	8	60	Quartz Mica Schist
22,700	2	8	90	Quartz Mica Schist
22,725	2	4	55	Quartz Mica Schist
22,750	4	18	79	Quartz Mica Schist
22,775	2	8	60	Quartz Mica Schist
22,825	140	25	60	Andalusite Schist
22,860	10	5	60	Quartz Mica Schist
22,870	10	3	65	Quartz Mica Schist

Q - quartz, An - Andalusite, i - with, Ret - retrograde, Mi - Mica, Sc - schist, Fe - iron, Veil - veinlet.

Cu-Pb-Zn Values from South Hill Drill Hole 1

Depth in Feet	Cu	Pb	Zn	Sample Description
187	122	26	142	Garnet rich biotite schist
210	118	28	147	Biotite Schist
223	6	30	131	Quartz Mica Schist
262	22	50	173	Andalusite Schist i coarse garnets
315	19	38	110	Ret. Andal. Schist i garnets
330	24	40	50	Biotite Schist i ret andalusites
348	12	64	155	Biotite Schist i ret andalusites
380	24	36	95	Biotite Schist i ret andalusites
397	70	22	71	Biotite Schist i ret andalusites
415	190	12	35	Biotite Schist - garnetiferous
446	259	18	119	Quartz Mica Schist
470	21	28	168	Biotite Schist i fine andalusites
497	14	18	77	Quartz Mica Schist
524	12	40	49	Andalusite Schist
532	11	22	23	Quartz Mica Schist
572	125	26	35	Quartz Mica Schist
587	68	22	38	Biotite Schist
607	33	32	173	Quartz Mica Schist i andalusites
635	36	20	104	Quartz Mica Schist
652	39	30	82	Biotite Schist i andalusites
670	15	48	89	Quartz Mica Schist

i - with, ret - retrograde

Wheal Ellen Drill Hole No. 7 Northern Mining

Sample Depth in Feet	Cu ppm	Pb ppm	Zn ppm	Sample Description
200-205	35	25	290	Quartz-mica schist
205-210	40	40	450	Andalusite schist
210-215	30	30	450	
215-220	30	90	2,400	
220-225	40	600	2,500	
225-230	20	900	1,200	
230-235	20	620	1,300	Pyritic schist
235-240	40	800	1,900	
240-245	40	870	1,600	
245-250	40	320	1,100	
250-255	50	120	310	
255-260	40	35	210	
260-265	45	<20	170	
265-270	50	<20	120	
270-275	55	35	170	
275-280	25	25	330	
280-285	30	<20	230	
285-290	30	20	180	Quartz-mica schist
290-295	30	<20	90	
295-300	40	<20	85	
300-305	50	<20	60	
305-310	30	20	90	
310-315	20	<20	2,000	Pyritic schist
315-320	35	20	240	
320-325	20	<20	100	
325-330	20	<20	100	
330-335	50	20	100	
335-340	30	<20	100	
340-345	60	20	95	
345-350	40	<20	130	Quartz-mica schist
350-355	20	20	120	
355-360	25	<20	70	
360-365A	30	25	110	
360-365B	20	35	160	
365-370	50	30	90	

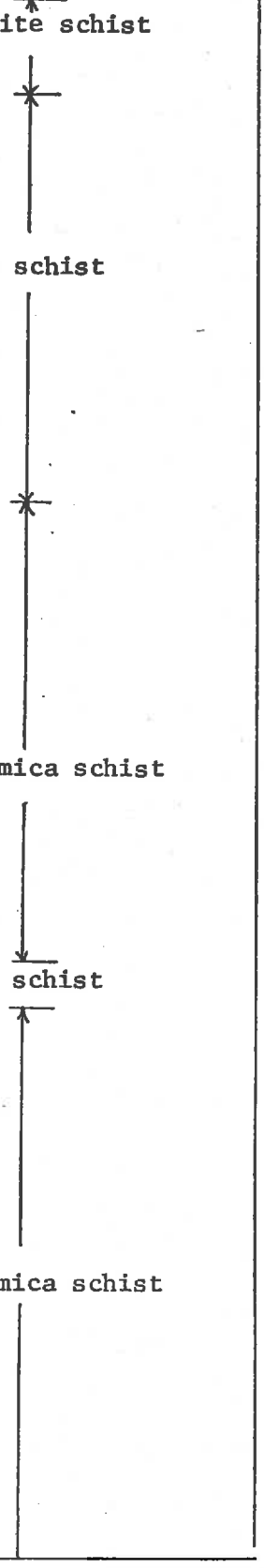

Wheal Ellen Drill Hole No. 7 Northern Mining

Sample Depth in Feet	Cu ppm	Pb ppm	Zn ppm	Sample Description
370-375	20	20	250	
375-380	20	30	110	
380-385	25	<20	100	
385-390	20	20	90	
390-395	25	<20	100	
395-400	30	<20	110	
400-405	35	<20	120	Quartz-mica schist
405-410	30	40	140	
410-415	20	35	140	
415-420	20	20	140	
420-425	40	20	130	
425-430	25	25	190	
430-435	40	20	250	Pyritic schist
435-440	40	20	460	
440-445	20	20	120	Andalusite schist
445-450	65	<20	80	
450-455	25	<20	70	
455-460	10	<20	50	
460-465	10	<20	60	Quartz-mica schist
465-470	10	<20	50	
470-475	10	<20	50	
475-480	120	<20	50	
480-485	10	<20	45	
485-490	20	<20	75	
490-495	10	<20	60	
495-500	60	20	65	
500-505	60	120	190	
505-510	45	60	95	
510-515	15	40	70	
515-520	30	80	120	
520-525	20	45	130	
525-530	10	35	50	
530-535	10	40	55	
535-540	30	40	70	
540-545	15	25	65	

Wheal Ellen Drill Hole No. 7 Northern Mining

Sample Depth in Feet	Cu ppm	Pb ppm	Zn ppm	Sample Description
545–550	10	25	110	Quartz-mica schist
550–555	50	80	130	Pyritic schist
555–560	10	50	200	
560–565	5	25	80	
565–570	5	20	80	
570–575	30	25	75	
575–580	10	25	100	
580–585	10	20	85	
585–590	20	25	130	
590–595	70	25	130	
595–600	20	25	150	
600–605	15	30	90	
605–510	45	30	95	
610–615	5	25	85	
615–620	20	30	80	
620–625	20	25	90	
625–630	5	30	100	
630–635	40	40	200	
635–640	20	50	260	Quartz-mica schist
640–645	10	20	90	
645–650	30	75	280	
650–655	30	30	90	
655–660	2	<30	60	
660–665	10	25	50	
665–670	10	25	45	
670–675	120	20	30	
675–680	150	25	45	
680–685	60	25	50	
685–690	45	25	60	
690–695	2	35	75	
695–700	2	<20	80	Andalusite schist
700–705	10	30	85	
705–710	50	70	230	
710–715	130	250	350	
715–720	40	25	45	

Wheal Ellen Drill Hole No. 7 Northern Mining

Sample Depth in Feet	Cu ppm	Pb ppm	Zn ppm	Sample Description
720-725	30	30	40	Andalusite schist
725-730	180	20	35	
730-735	170	20	25	
735-740	10	25	45	
740-745	320	25	75	
745-750	10	20	50	
750-755	30	20	65	
755-760	85	20	55	
760-765	55	20	50	Quartz-mica schist
765-770	25	20	40	
770-775	10	20	50	
775-780	2	<20	50	
780-785	2	<25	60	
785-790	20	20	40	
790-795	10	25	50	
795-800	15	25	65	
800-805	10	20	35	
805-810	20	20	40	
810-815	10	20	45	
815-820	15	620	330	
820-825	10	160	65	Andalusite schist
825-830	10	240	75	
830-835	10	75	50	
835-840	10	80	40	
840-845	10	60	40	
845-850	5	55	40	
850-855	10	85	40	
855-860	40	30	40	
860-865	10	25	30	
865-870	10	20	30	
870-875	20	20	30	
875-880	35	65	50	
880-885	150	25	25	
885-890	140	35	30	Quartz-mica schist
890-895	.....Sample missing....			

Wheal Ellen Drill Hole No. 7 Northern Mining

Sample Depth in Feet	Cu ppm	Pb ppm	Zn ppm	Sample Description
895–900	120	20	30	
900–905	220	20	20	
905–910	250	20	30	
910–915	240	20	45	
915–920	130	30	30	
920–925	20	25	30	
925–930	20	20	50	
930–935	10	25	30	
935–940	2	25	35	
940–945	10	20	30	
945–950	55	20	30	
950–955	10	20	30	
955–960	10	20	30	
960–965	10	20	25	
965–970	5	20	30	
970–975	5	20	30	
975–980	5	25	20	
980–985	15	60	30	
985–990	10	25	20	

APPENDIX 4

Whole Rock Analyses

Four whole rock analyses were made by x-ray fluorescence. Two andalusite schists and two pyritic schists were analysed to compare with the results of previous workers Lindqvist (1969) and George (1967). Andalusite schist values suggest the original sediments to be a shale (Pettijohn, 1957) while the pyritic schist values even though different to the Nairne Pyrite Horizon (George, op. cit.) were probably Fe rich shales.

Fused buttons were made using material preheated to 110°C for two hours and for a further 12 hours to 1000°C. Weight loss was determined from the heated sample and represents the sum of:

S, C, H_2O^+, H_2O^- and $Fe^{2+} \rightarrow Fe^{3+}$

The relatively low weight loss observed for the pyritic schist is probably due to the balance of weight reduction by volatiles (S, C, H_2O^+ and H_2O^-) with weight increase in transforming Fe^{2+} to Fe^{3+}.

Sodium analyses were measured using a flame photometer.

APPENDIX 5

Modal Analyses

A description of the important mineral assemblages and textures were given in section 4 (Metamorphism) and 5 (Mineralization). Modal analyses (visual) of those samples housed (thin sections, polished-thin sections) in the geology department are as follows on the following page.

Q	quartz	Ms	muscovite	Bi	biotite
An	andalusite	St	staurolite	Cl	chlorite
Gn	garnet	Fi	fibrolite	Cp	chalcopyrite
Py	pyrite	Sp	sphalerite	Po	pyrrhotite
Il	ilmenite	Mk	mackinawite	Mc	marcasite
Mg	magnetite	Cc	chalcocite	Pl	plagioclase
Cpx	clinopyroxene	Am	amphibole	Cd	cordierite
Opq	opaques	Sc	schist	Cal	calc-
Sil	silicate				

THIN SECTIONS

Sample No.	Q	Bi	Ms	Gn	An	St	Cl	Pl	cpx	Am	Fi	Cd	opq	Lithology
501/003	2	30	8	Tr	48			Tr			10		2	An.Sc
501/004	20	40	5	1	30						4		Tr	An.Sc
501/005	20	35	24		20						1		Tr	An.Sc
501/006	61			5				?	17	20			2	Cal.Sil
501/011	35		60										5	Py.Sc
501/013		25	Tr	12		60	Tr						3	Gn.Sc
501/014	52	30	2	1	15									An.Sc
501/015	50	25	12		10								3	An.Sc
501/016	50	35	3	10			Tr						2	Bi.Sc
501/017	65	15	15	Tr	5						Tr		Tr	An.Sc
501/018	58	10	8	2	8	5	5				1		3	Gn.Cl.Sc
501/021	35	45	8	1	10		Tr						1	An.Sc
501/022	35	45	3		15		Tr						2	An.Sc
501/025	70	15	15										Tr	Q.Mi.Sc
501/026	65	20	15										Tr	Q.Mi.Sc
501/065		44	2	35	1	13	5							Gn.Cl.Sc
501/067	30	46	5		15						2		2	An.Sc
501/067b	30	50	4		15						1			An.Sc
501/069	25	53	5		15			1			Tr		1	An.Sc
501/071	43	20	20	1	5		10				1			An.Sc
501/074	47	35	5	3	2	5	1				1		1	Bi.Sc

Thin Sections (cont.)

Sample No.	Q	Bi	Ms	Gn	An	St	Cl	Pl	Cpx	Am	Fi	Cd	opq	Lithology
501/076	55	20		20									5	Bi.Sc.
501/077						30	60						10	Gn.Cl.Sc.
501/100		40						35		20	3		2	Cal.Sil.
501/101	8	2		40			10			30		10		Cal.Sil.
501/104	53	20		8	15	Tr	1				Tr		3	An.Sc.

Polished-thin sections

Sample No.	Q	Ms	Bi	An	St	Cl	Gn	Fi	Cp	Py	Sp	Po	Il	Mk	Mc	Mg	Cc
501/126	40	Tr	29	2	8	1	10	Tr	5	2	Tr	Tr	Tr	Tr	Tr	3	
501/129	50		15	1	Tr	6	13	Tr	7	4	Tr		2	Tr		2	
501/132	44	10	24	2		4	2	2	7	2			Tr			Tr	3
501/133	70	5	8	5			1	Tr	4	4			1		1	1	
501/134	31		30		8	1	10		8	8	Tr	Tr	1	Tr	1	2	

Wheal Ellen

Cpy - chalcopyrite Py - pyrite Gn - galena Sp - sphalerite
Po - pyrrhotite T - tetrahedrite Mc - marcasite As - arsenopyrite
Gb - galenobismutite Mg - magnetite Ilm - ilmenite G - gahnite
Gan - gangue Tr - trace Bl - boulangerite

Wheal Ellen — Polished-sections

Sample No.	Cpy	Py	Gn	Sp	Po	T	Mc	As	Gb	Bl	Mg	Ilm	G	Gan
501/035		2	30	68	Tr									
501/036	Tr	7	20	65	Tr	1	3		1		Tr	Tr	Tr	3
501/037		5	20	65	1	1	Tr		1					7
501/038		Tr	7	Tr	Tr	Tr			Tr					93
501/060	14	60	1	25	Tr	Tr								
501/061	1	5	4	45			Tr							45
501/064	17	8		60	1		4							10
501/109			1										90	9
501/110	Tr	45	5	49		Tr	1							
501/113		9	10	80	Tr	1								
501/115		4	7										1	89
501/122		Tr	30	67	1	2		Tr						
501	Tr	13	80			2				5				
WE4 358	52	45		3	Tr	Tr					Tr	Tr		
WE4 360	1	30	6	1				2			Tr	Tr		60

South Hill

Cpy - chalcopyrite Py - pyrite Sp - sphalerite Po - pyrrhotite
Mk - mackinawite Mc - marcasite Cc - chalcocite Mg - magnetite
Ilm - ilmenite Gan - gangue Tr - trace

South Hill — Polished-sections

Sample no.	Cpy	Py	Sp	Po	Mk	Mc	Cc	Mg	Ilm	Gan
501/039		98	1	1				Tr		
501/046	44	25	5	1	1	20		2	2	
501/047	55	3	3	2	1					36
501/048	30	30					Tr	10	30	
SH4 263	51	8	Tr	Tr			40	Tr	1	

Bremer

Cpy - chalcopyrite Py - pyrite Po - pyrrhotite Mk - mackinawite
Mc - marcasite Cv - covellite Mg - magnetite Ilm - ilmenite
Gan - gangue Fe - limonite and goethite Tr - trace
Sp - sphalerite

Bremer — Polished-sections

Sample No.	Cpy	Py	Sp	Po	Mk	Mc	Cv	Mg	Ilm	Fe	Gan
501/042	40	42	2	Tr	Tr			1	10	5	
501/043	45	8	Tr		1		1			15	30
501/044	63	1	Tr	Tr	1					5	30
501/125	91	2	1	Tr	Tr						6

Kanmantoo Area

Cpy - chalcopyrite
Py - pyrite
Sp - sphalerite
Po - pyrrhotite
Mk - mackinawite
Bis - bismuth
Bit - bismuthinite
Au - gold
Cb - cubanite
Mg - magnetite
Ilm - ilmenite
Fe - limonite and goethite
Tr - trace
Gan - gangue

Kanmantoo Area — Polished-sections

Sample No.	Cpy	Py	Sp	Po	Mk	Bis	Bit	Au	Cb	Mg	Ilm	Fe	Gan
501/050	80	3	Tr		Tr	1	Tr		1				15
501/052	15	5	Tr	Tr	Tr	Tr	1	Tr	1	Tr	3		75
501/053	72	8	Tr	Tr	Tr				Tr	Tr	Tr		20
501/054	5	3	Tr	Tr	Tr					Tr	2		90
501/055	30	5	Tr	Tr	Tr						Tr		65
KS 104	34	9	Tr	Tr	Tr		Tr			3	2		53
KS 104 2135	22	3	Tr	Tr	Tr	5	Tr			3	2		65
KS 104 2143	25	6	Tr	Tr	Tr	5				2	2		60

Strathalbyn

Cpy - chalcopyrite
Py - pyrite
Ilm - ilmenite
Mg - magnetite
As - arsenopyrite
T - tetrahedrite
Po - pyrrhotite
Mc - marcasite
Sp - sphalerite
Gan - gangue
Tr - trace

Strathalbyn — Polished-sections

Sample No.	Cpy	Py	Ilm	Mg	As	T	Po	Mc	Sp	Gan
501/056		1			24	Tr	Tr			75
501/057	Tr	45		1	Tr			10		44
501/058	2	39		2			2			55
ST1 207	1	57	1	Tr	1		Tr		Tr	40
ST1 218	Tr	45		Tr			Tr	Tr		55

APPENDIX 6

Study Procedure

The work done included:

(a) mapping and a detailed literature study in two periods, December 1975 - February 1976 and April - October, 1976.

(b) study of approximately 90 polished thin sections, 10 polished sections and 80 thin sections.

(c) preparation and analyses of (1) 50 sulphur dioxide samples for a sulphur isotope study, (2) 54 samples for Cu-Pb-Zn content, and (3) 4 samples for whole rock values.

(d) study of 15 electron microprobe samples of sphalerite.

SOUTH HILL PROSPECT

LEGEND

- ANDALUSITE SCHIST
- QUARTZ MICA / BIOTITE SCHISTS
- GARNET CHLORITE SCHIST
- PYRITIC SCHIST
- QUARTZ VEINS q
- CALC SILICATE c

- BEDDING (S_o)
- SCHISTOSITY (S_1)
- MINERAL LINEATION (L_1)
- CRENULATION LINEATION (L_2)
- CRENULATION LINEATION (L_3)

- Lithological Boundary
- Sample *soil*
- Fence
- Pit
- Highway Cutting, Road, Track
- Building
- Dam
- Stream
- Suboutcrop
- oS7 Drill Hole

0 metres 200

N

SCALE 1:4000

FIG. 2

SPRY 1976

WHEAL ELLEN

LEGEND

- QUART MICA / BIOTITE SCHISTS
- ANDALUSITE SCHIST
- INTERBANDED ANDALUSITE–BIOTITE SCHIST
- GARNET CHLORITE SCHIST
- GARNET SANDSTONE
- CALC SILICATE
- PYRITIC SCHIST
- QUARTZ VEINS

- BEDDING (S_o)
- SCHISTOSITY (S_1)
- MINERAL LINEATION (L_1)
- CRENULATION LINEATION (L_2)
- AXIAL PLANE (S_4)

- Lithological Boundary
- Sample so/025
- Fence; Wall
- Pit
- Road
- Costean
- Building
- Stream
- Surface Dump
- Shaft
- oW3 Drill Hole

N

SCALE 1:4000

FIG.3

0 metres 200

SPRY 1976